Journal Pre-proof

Novel 2, 5-diketopiperazine derivatives as potent selective histone deacetylase 6 inhibitors: Rational design, synthesis and antiproliferative activity

Xin Chen, Xinyang Chen, Raphael R. Steimbach, Tong Wu, Hongmei Li, Wenjia Dan, Peidong Shi, Chenyu Cao, Ding Li, Aubry K. Miller, Zhixia Qiu, Jinming Gao, Yong Zhu

PII: S0223-5234(19)31102-X

DOI: https://doi.org/10.1016/j.ejmech.2019.111950

Reference: EJMECH 111950

To appear in: *European Journal of Medicinal Chemistry*

Received Date: 5 July 2019

Revised Date: 5 November 2019

Accepted Date: 2 December 2019

Please cite this article as: X. Chen, X. Chen, R.R. Steimbach, T. Wu, H. Li, W. Dan, P. Shi, C. Cao, D. Li, A.K. Miller, Z. Qiu, J. Gao, Y. Zhu, Novel 2, 5-diketopiperazine derivatives as potent selective histone deacetylase 6 inhibitors: Rational design, synthesis and antiproliferative activity, *European Journal of Medicinal Chemistry* (2020), doi: https://doi.org/10.1016/j.ejmech.2019.111950.

GRAPHICAL ABSTRACT

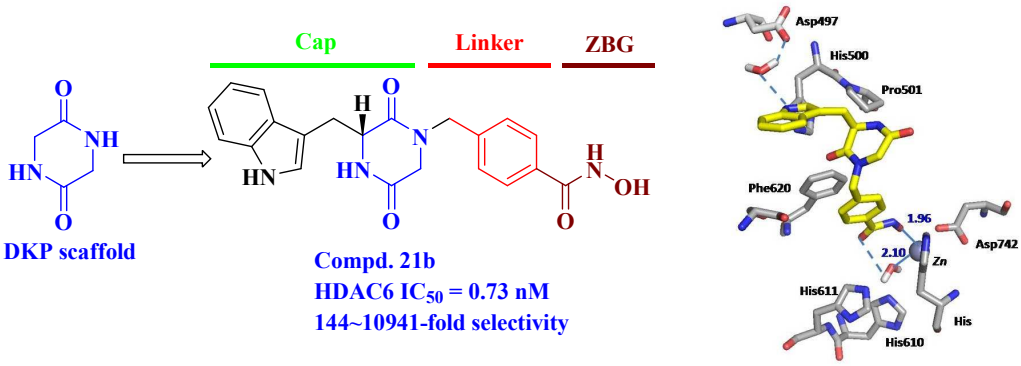

Novel 2, 5-Diketopiperazine Derivatives as Potent Selective Histone Deacetylase 6 Inhibitors: Rational Design, Synthesis and Antiproliferative Activity

Xin Chen[a], Xinyang Chen[a], Raphael R. Steimbach[b, c], Tong Wu[a], Hongmei Li[d], Wenjia Dan[a], Peidong Shi[a], Chenyu Cao[a], Ding Li[a], Aubry K. Miller[b, e], Zhixia Qiu[f], Jinming Gao[a,*], Yong Zhu[d,*]

[a]*Shaanxi Key Labotory of Natural Products & Chemical Biology, College of Chemistry & Pharmacy, Northwest A&F University, Yangling 712100, P. R. China*

[b]*Cancer Drug Development Group, German Cancer Research Center (DKFZ), 69120 Heidelberg, Germany*

[c]*Biosciences Faculty, University of Heidelberg, 69120 Heidelberg, Germany*

[d]*School of Science, China Pharmaceutical University, Nanjing, 210009, P. R. China*

[e]*German Cancer Consortium (DKTK), 69120 Heidelberg, Germany*

[f]*School of Traditional Chinese Pharmacy, China Pharmaceutical University, Nanjing, 210009, P. R. China*

Corresponding Author

*Jinming Gao

E-mail: jinminggao@nwsuaf.edu.cn; Fax: +87-29-87092335

*Yong Zhu

E-mail: zhuyong@cpu.edu.cn; Fax: +86-25-86185182

Notes

The authors declare no competing interest.

Abstract

Histone deacetylase 6 (HDAC6) has gained popular attention for its wide participation in various pathological process recently. In this paper, a series of novel derivatives containing 2, 5-diketopiperazine (DKP) skeleton were developed as potent selective HDAC6 inhibitors (sHDAC6is). Most of these compounds exhibited low nanomolar IC_{50} values toward HDAC6, and the best compound was **21b** (IC_{50} = 0.73 nM) which had 144~10941-fold selectivity over other HDAC isoforms. Western blot assay further validated these compounds to be sHDAC6is. Molecular simulation of **21b** was conducted to rationalize the high binding affinity for HDAC6. In the cytotoxicity experiment, **18a**, **18b** and **18d** gave superior or comparable influence on the growth of two multiple myeloma cells U266 and RPMI-8226 compared to ACY-1215. Moreover, the combination of **18a** and adriamycin showed synergistic effect against non-small cell lung cancer cell A549. **18a** and **18b** also demonstrated appropriate drug metabolism in human liver microsome (HLM).

Key words:

HDAC6 inhibitor; DKP; Selectivity; Synthesis; Combination therapy

1. Introduction

Protein lysine acetylation is a reversible posttranslational modification that is balanced by histone acetyltransferases (HATs) and histone deacetylases (HDACs)[1]. During the past decades, HDACs as promise targets had been studied extensively[2]. However, a lot of clinical trials indicate that the use of pan-HDACis leads to undesirable side effects, such as fatigue, diarrhea, nausea, thrombocytopenia, and cardiotoxicity[3-5]. The application of broad spectrum or class I selective HDACis is limited because of a narrow therapeutic window[6]. A common view is that developing isoform-selective HDAC inhibitor (HDACi) would be advantageous over pan-HDACis for lower toxicity and improved safety profile[7]. In contrast with the lethal effect of HDAC1-3

genetic ablation, mice with HDAC6-knocked out are viable and develop normally[8]. Among all the 11 Zn^{2+}-dependent HDAC members, HDAC6 consists of 1216 aa and uniquely has two functional domains, a dynein motor binding domain and a zinc finger domain. HDAC6 is mainly localized in cytoplasm and plays an important role in microtubule dynamics and chaperone activities[9]. The major substrates of HDAC6 are non-histone proteins including α-tubulin, Hsp90, cortactin and peroxiredoxin, and this makes HDAC6 involved in many cellular processes such as motility, adhesion, migration, growth of cells, immune synapse formation, and stress granule formation[10, 11]. Moreover, HDAC6 is found to be highly expressed in many diseases including tumors and neurological diseases; inhibition of HDAC6 suppresses microtubule dynamics and results in cell cycle arrest and apoptosis, making HDAC6 become an attractive drug target in cancer therapy[12-14].

By so far, a lot of HDAC6is have been reported such as ricolinostat (ACY-1215)[15], HPOB[16], tubastatin A[17] and et al[18-20], and they also have common pharmacophores: cap, linker and zinc binding group (ZBG). However, the development of potent and efficient sHDAC6is for clinical treatment is still urgent. The intrinsic biocompatibility and affinity for target binding of peptides have attracted chemists to obtain peptide inhibitors with improved HDAC isoforms selectivity. The most famous peptide-based HDACis are cyclic tetrapeptides equipped with active Zn^{2+} binding groups, such as the approved drug FK228 which displays class I selectivity[21]. Recently, the use of peptide or peptoid as the capping group of HDACis arouses great interest (**Fig. 1**). Compound **1** is a substrate mimic based on the histone H4 tail which incorporates a hydroxamic acid functionality, and inhibits HDAC1 with an IC_{50} of 336 nM[22]. Compound **2** containing a peptoid capping group exhibits strong inhibition of HDAC1-3 and HDAC6[23]. The dual HDAC-proteasome inhibitor **3**, inhibits both HDAC6 and the chymotrypsin-like proteasome, and shows potent and selective anticancer activity[24]. Trapoxin A (**4**), a microbial cyclic tetrapeptide, is an essentially irreversible inhibitor of HDAC8, with Kd value of 3 nM[25].

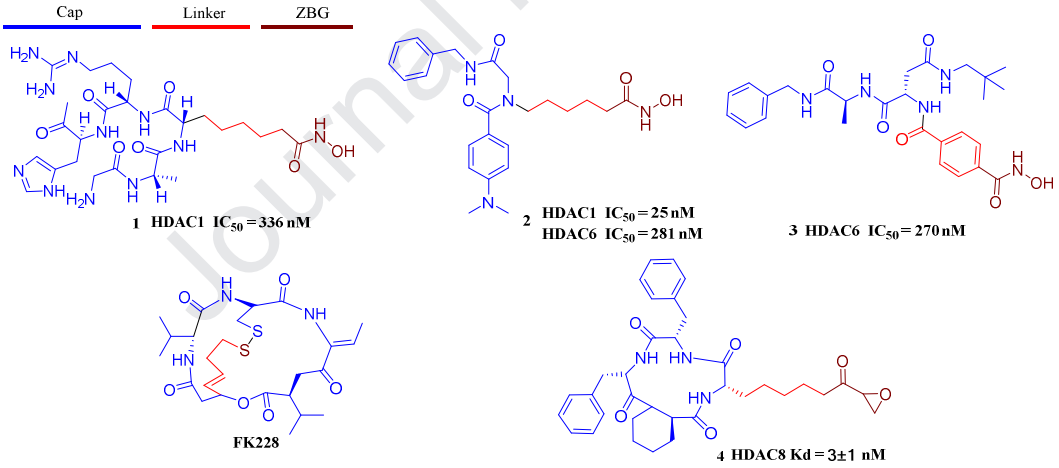

Fig. 1 Reported peptide or peptoid HDAC inhibitors.

In consideration of the flexible conformation and instable physical and metabolite properties of peptides, a conformation-restricted HDAC-interacting peptide bearing the ZBG group might provide a suitable scaffold for novel HDACis. Wang et.al reported a series of stabilized peptide HDACis derived from HDAC1 substrate H3K56 which exhibited significantly increased safety window and better selectivity toward malignant cells than SAHA[26]. Then, an inflexible capping group may improve selectivity against HDAC6 [27-29]. In present study, we cyclized two adjacent peptide bonds (as exemplified by compound **1**) into the rigid 2, 5-diketopiperazine scaffold which exists in numerous bioactive natural products[30] and introduced the phenylhydroxamic acid group, a key pharmacophore of sHDAC6i, to the N-1 of the DKP skeleton, producing a series of novel 1, 3-disubstituded or 1, 3, 4-trisubstituded DKP derivatives (**Fig. 2**). Here, we reported the synthesis, structure and activity relationship (SAR) study and anticancer evaluation of these derivatives.

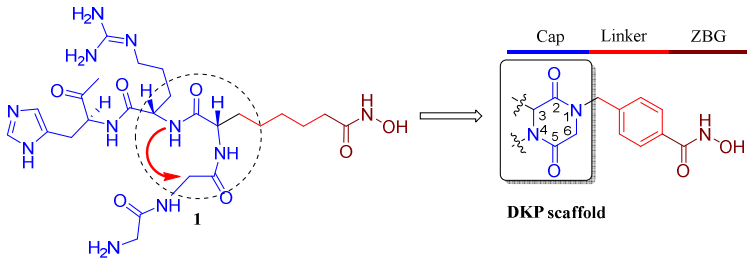

Fig. 2 The design of novel DKP derivative as selective HDAC6 inhibitors.

2. Results and discussion

2.1 *Chemistry*

Although a lot of reports had described diverse synthesis of the DKP scaffold, a concise and convenient synthetic procedure for 1, 3-disubstituted DKP is still rare, according to our literatures review. Here, we efficiently constructed the 1, 3-disubstituted DKP skeleton through an one-pot synthesis in three steps from amino ester, chloroacetyl chloride and substituted benzylamine in a good overall yield (**Fig.3**). The representative synthetic process was as follows: (a) Amidation of amino ester with chloroacetyl chloride yielded intermediate **A**, using triethylamine (Et_3N) as the base and acetonitrile as the solvent. (b) Methyl 4-(aminomethyl)benzoate was added to give intermediate **B** when the temperature was ascending to reflux. (c) The mixture was concentrated in vacuo to remove extra Et_3N and 10% silica gel was subsequently added to enhance the conversion of **B** to the cyclized 1, 3-disubstituted DKP skeleton.

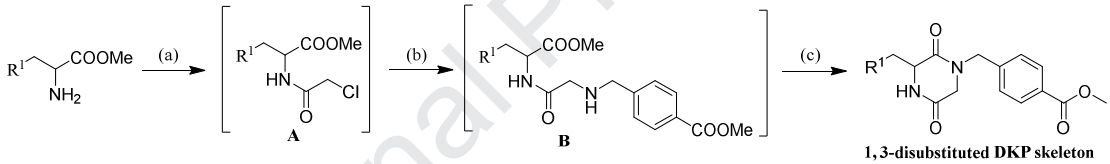

Fig 3. One-pot synthesis in three steps for 1, 3-disubstituted DKP skeleton.

At the beginning, the phenyl was chosen as the capping group because it was applied widely in many HDACis. Stereochemistry of medicinal molecular had an important impact on pharmacological activity. Hence, we synthesized both *S*- and *R*-configuration enantiomers **11a** and **11b** to investigate the effect of the C-3 chirality on HDAC6 activity. The synthetic routes of compounds **11a-b** were displayed in **Scheme 1**. Key DKP intermediates **8a-b** were synthesized following the one-pot procedure using **7a-b** as starting materials. Hydrolysis of **8a-b** in the presence of sodium hydroxide at room temperature afforded **9a-b**. Amidation of **9a-b** with *O*-(tetrahydro-2*H*-pyran-2-yl) hydroxylamine by 2-(7-Aza-1*H*-benzotriazole-1-yl)-1, 1, 3, 3-tetramethyluronium hexafluorophosphate (HATU) gave **10a-b**. Deprotection of **10a-b** in methanol with the catalytic *p*-TsOH·H_2O furnished target compounds **11a-b**.

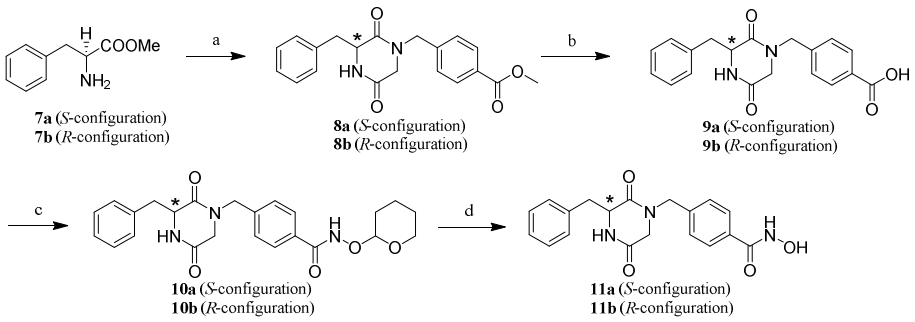

Scheme 1. Reagents and conditions: (a) 1. CH_3COCl, Et_3N, acetonitrile, 0 °C, 1 h; 2. Methyl 4-(aminomethyl)benzoate hydrochloride, acetonitrile, reflux, 6 h; 3. 10% silica gel, reflux, overnight; (b) NaOH, THF/water (v/v) = 1:1, r.t., overnight; (c) HATU, *N*,

N-diisopropylethylamine (DIPEA), *N*, *N*-dimethylformamide (DMF), *O*-(tetrahydro-2*H*-pyran-2-yl) hydroxylamine, r.t., 6 h; (d) *p*-TsOH·H_2O, MeOH, overnight.

To explore the SAR of ZBG group on different positions of phenyl linker, compound **13** with hydroxamic acid on the *m*-position of phenyl linker was synthesized according to the method described in **Scheme 1** with starting material **7a**.

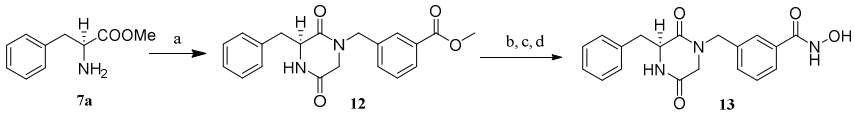

Scheme 2. Reagents and conditions: (a) 1. CH_3COCl, Et_3N, acetonitrile, 0 °C, 1 h; 2. Methyl 3-(aminomethyl)benzoate hydrochloride, acetonitrile, reflux, 6 h; 3. 10% silica gel, reflux, overnight; (b) NaOH, THF/water (v/v) = 1:1; (c) HATU, DIPEA, DMF, *O*-(tetrahydro-2*H*-pyran-2-yl) hydroxylamine, r.t., 6 h; (d) *p*-TsOH·H_2O, MeOH, overnight.

Racemic compounds **15a-c** were synthesized to preliminarily show the effect of different substituents on N-4 position of DKP on enzymatic activity. As showed in **Scheme 3**, nucleophilic reactions of **8a** with various alkyl halides gave intermediates **14a-c** with sodium hydride (NaH) as the base. Then **14a-c** were treated following the same procedure as **8a-b** to give desired compounds **15a-c**.

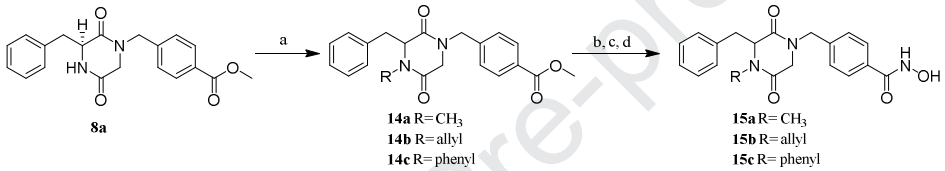

Scheme 3. Reagents and conditions: (a) NaH, anhydrous tetrahydrofuran (THF), 60 °C, various alkyl halides, 3 h; (b) 1. CH_3COCl, Et_3N, acetonitrile, 0 °C, 1 h; 2. Methyl 4-(aminomethyl)benzoate hydrochloride, acetonitrile, reflux, 6 h; 3. 10% silica gel, reflux, overnight; (c) NaOH, THF/water (v/v) = 1:1; (d) HATU, DIPEA, DMF, *O*-(tetrahydro-2*H*-pyran-2-yl) hydroxylamine, r.t., 6 h; (e) *p*-TsOH·H_2O, MeOH, overnight.

Based on the SAR of compounds **11a**, **11b** and **15a-c**, *R*-configuration compounds **18a-e** with different substituents on N-4 position of DKP were synthesized. As shown in **Scheme 4**. Compound **7b** was treated with various aldehydes to afford Schiff's bases, which were then in-situ reduced with sodium cyanoborohydride ($NaBH_3CN$) to generate intermediates **16a-e**. Subsequently, **16a-e** were reacted in the same procedure as shown in **Scheme 1** to give desired analogs **18a-e**.

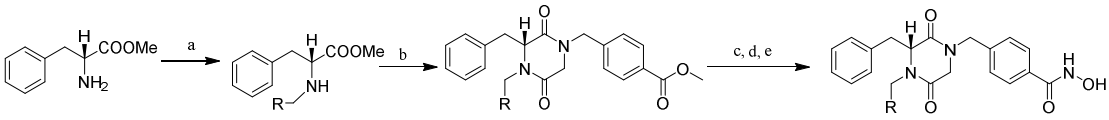

Scheme 4. Reagents and conditions: (a) 1. RCHO, r.t., 30 min; 2. MeOH, $NaBH_3CN$, 12 h; (b) 1. CH_3COCl, Et_3N, acetonitrile, 0 °C, 1 h; 2. Methyl 4-(aminomethyl)benzoate hydrochloride, acetonitrile, reflux, 6 h; 3. 10% silica gel, reflux, overnight; (c) NaOH, THF/water (v/v) = 1:1; (d) HATU, DIPEA, DMF, *O*-(tetrahydro-2*H*-pyran-2-yl) hydroxylamine, r.t., 6 h; (e) *p*-TsOH·H_2O, MeOH, overnight.

Besides, compounds **21a-b** with indolyl capping group were also synthesized. By means of the same procedure as **11a-b**, compounds **21a-b** were made from starting materials **19a-b**, as described in **Scheme 5**.

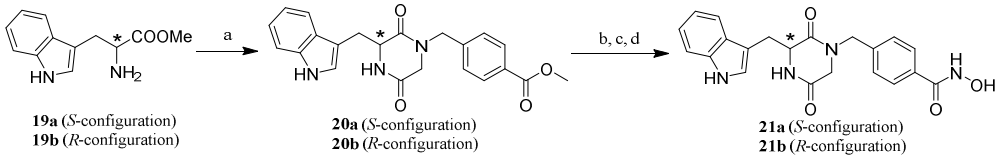

Scheme 5. Reagents and conditions: (a) 1. CH_3COCl, Et_3N, acetonitrile, 0 °C, 1 h; 2. Methyl 4-(aminomethyl)benzoate hydrochloride, acetonitrile, reflux, 6 h; 3. 10% silica gel, reflux, overnight; (b) NaOH, THF/water (v/v) = 1:1; (c) HATU, DIPEA, DMF, *O*-(tetrahydro-2*H*-pyran-2-yl) hydroxylamine, r.t., 6 h; (d) *p*-TsOH·H_2O, MeOH, overnight.

2.2 *HDAC inhibition and SAR study of the target compounds*

All prepared compounds were examined for their inhibitory ability against HDAC6, using Trichostatin A (TSA, a pan-HDAC inhibitor) and HPOB (sHDAC6i) as the positive controls. The preliminary selective profile toward HDAC1 and HDAC8 were evaluated to guide the structural modification. IC_{50} values for inhibition of these isoforms along with selectivity are summarized in **Table 1**. (*S*)-isomer **11a** bearing a phenyl capping group, preferentially inhibited HDAC6 and HDAC8 (IC_{50}, 17.5 and 15.6 nM respectively) with HDAC1 activity merely in the micromolar range. Interestingly, by simply "switching" the chirality, the *R* stereoisomer **11b** was 2-fold more active than **11a** on HDAC6 inhibition (IC_{50} = 8.62 nM). In addition, **11b** also improved selectivity toward HDAC6 versus HDAC1 (959-fold) and HDAC8 (4-fold). The shift of hydroxamic acid ZBG from C-4 to C-3 of the phenyl linker (compound **11a** vs **13**) led to a sharp decrease of HDAC6 inhibitory potency and complete loss of HDAC1 and -8 activities.

To our delight, racemic analogues **15a-c** with different substituents on N-4 of DKP scaffold retained enzymatic inhibitory potency. Methyl or phenyl substituent had a little better HDAC6 inhibitory activity than that of allyl group, with IC_{50} values of 16.7, 16.3 and 25.4 nM, respectively. This result revealed that the cavity of protein around N-4 of DKP could tolerate substitutions with various steric hindrances. Subsequently, further structural modification of N-4 was performed based on **11b** which had a better HDAC6 activity and selectivity. Compared to **11b**, compounds **18a-e** with unsubstituted or substituted phenyl groups (-Cl and -OMe) all had slightly reduced activities against HDAC6 with IC_{50} values in double-digit nanomolar range, but superior selectivity over HDAC8. As shown in **18b-d**, the relative positions of the -Cl substituent on the phenyl had no obvious impact on activities.

The HDAC6 inhibitory activities were markedly influenced by substituents on C-3 position of DKP. Replacement of the phenyl capping group with 3-indolyl substitution led to a 2.6-fold improvement of HDAC6 inhibition (**21a** vs **11a**, IC_{50} = 6.64 and 16.7 nM, respectively). In comparison with **21a**, the *R*-stereoisomer **21b** exhibited more than 9-fold better activity against HDAC6 with an IC_{50} value of 0.73 nM, and this trend was consistent with those of **11a** and **11b**. Moreover, **21b** exhibited nearly 10941-fold selectivity versus HDAC1 and 700-fold selectivity versus HDAC8. Compared to the sHDAC6 inhibitors HPOB (IC_{50} = 33.78 nM) and Tubastatin A (IC_{50} = 15 nM), **21b** also had 46-fold and 21-fold better enzymatic inhibitions on HDAC6 respectively, and showed higher selectivity over HDAC1 and HDAC8.

Table 1 Inhibitory Profile of DKP Derivatives and Trichostatin A (TSA) against Human HDAC1, -6, and -8 (IC_{50}, nM).

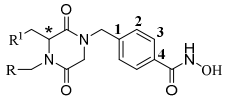

11a-b, 15a-c, 18a-d, 21a-b

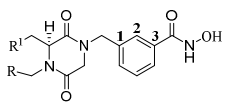

13

Compound	R	R^1	Isomer	IC_{50}[a]			selectivity	
				HDAC1	HDAC6	HDAC8	HDAC1/6	HDAC8/6
11a	H		*S*	7200± 51.92	17.50± 0.37	15.60 ± 0.40	411	0.9
11b	H		*R*	8270± 143.11	8.62± 0.41	30.90 ± 0.27	959	4
13	H		*S*	NA[b]	4190± 93.67	NA[b]	/	/
15a	CH_3		(*rac*)-	-[c]	16.70± 0.13	-	/	/
15b			(*rac*)-	-	25.40± 0.26	-	/	/

15c	Ph		(*rac*)-	-	16.30± 0.55	-	/	/
18a	Ph		*R*	9640.00±154.02	9.83± 0.21	145. 00± 2.10	981	15
18b	2-Cl-Ph		*R*	8310.00±126.33	10.10± 0.11	162.00± 1.03	823	16
18c	4-Cl-Ph		*R*	9200.00±225.25	11.70± 0.34	130.00± 1.16	786	11
18d	3-Cl-Ph		*R*	8550.00±193.67	10.50± 0.32	150.00± 2.14	838	14
18e	3-OCH_3-Ph		*R*	8100.00± 77.71	13.70± 0.09	171.00± 1.22	591	12
21a	H		*S*	6390.00±101.50	6.64± 0.13	112.00±1.96	962	17
21b	H		*R*	8020.00± 36.73	0.73± 0.02	513.00±13.17	10941	700
TSA	/	/	/	8.41± 0.25	5.56± 0.05	1160.00±49.90	1.5	209
HPOB	/	/	/	1780.00±67.20	33.78± 0.05	1990.00±98.50	53	59
Tubastatin A[d]	/	/	/	16400[d]	15[d]	854[d]	1093	57

[a]IC_{50} values for enzymatic inhibition of HDAC enzyme. We ran experiments in duplicate. Assays were performed by Reaction Biology Corporation (Malvern, PA, USA). [b]NA: no inhibition activity. [c]- : not tested. [d]values for Tubastatin A come from reference[16].

To probe the selectivity of these DKP derivatives versus the broader family of HDAC isotypes, the most potent compound **21b** was selected for full HDAC profiling at all the class I, II and IV HDACs with SAHA (an approved pan-HDACi) as the reference compound. As described in **Table 2**, **21b** exhibited distinct selectivity over class I HDAC1-3 (>10940-fold) and class IV HDAC11 (2456-fold). It also showed high level of selectivity over other class II HDACs (4, 5, 7, 9) reaching >1000-fold. HDAC8 was inhibited with an IC_{50} of 513 nM, and this might be contributed to its conformational flexibility to accommodate ligands with different structures including phenyl-linker compounds. Besides, a time-resolved fluorescence resonance energy transfer (TR-FRET) assay[31] was performed to test the HDAC10 inhibitory activities of **21b** and SAHA. **21b** inhibited HDAC10 with an IC_{50} value of 105 nM which was much weaker than that of HDAC6. These results established **21b** to be a potent and sHDAC6i.

Table 2

Complete characterization of **21b** at all 11 class I, II and IV HDAC enzymes (IC_{50}[a], nM).

Cpd.	**21b**	SAHA	Cpd.	**21b**	SAHA
HDAC1	8020±36.73	4.24±0.12	HDAC7	752.00±10.04	NA[b]
HDAC2	NA[b]	11.70±0.34	HDAC8	513.00 ±13.17	1020±27.34
HDAC3	NA[b]	3.05±0.09	HDAC9	2560±51.52	NA[b]
HDAC4	5620±178.56	NA[b]	HDAC10	105[c]	159[c]
HDAC5	4370±191.33	8750±126.78	HDAC11	1800±25.06	952.00 ±31.47
HDAC6	0.73± 0.02	7.10± 0.27			

[a]IC_{50} values for enzymatic inhibition of HDAC enzymes. We ran experiments in duplicate. Assays were performed by Reaction Biology Corporation (Malvern, PA, USA). [b]NA: no inhibitory activity. [c]HDAC10 activity was measured by the FRET assay.

2.3 *Western blot assay*

Acetylation of α-tubulin is an important epigenetic marker for HDAC6 inhibition. Western blot assay was performed to further validate the HDAC6 selectivity of the DKPs. HCT116 cells were treated with compound **21b**, SAHA and HPOB at 0.1, 1 and 10 μM for 24 h to measure the acetylation status of α-tubulin (HDAC6 dependent)

compared to total H3 acetylation (HDAC1-3 dependent) (**Fig. 4**). As expected, we observed a dose-dependent increase in the level of Ac-tubulin when the cells were treated with compound **21b**, but did not observe a significant increase in Ac-H3 even at 10 μM. In contrast, SAHA induced an increase in Ac-tubulin as well as an obvious increase in Ac-H3. These confirmed that cellular HDAC6 was selectively inhibited by the DKP **21b** in a robust manner.

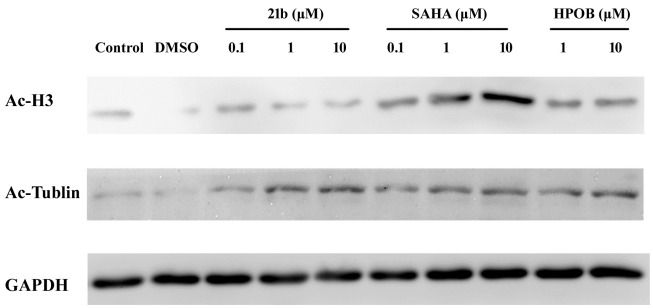

Fig. 4 Western blot of **21b** for Ac-H3 and Ac-Tub in HCT-116 cells with SAHA and HPOB as references.

2.4 *Molecular docking study*

Molecular simulation was performed to understand the interaction between the DKPs and protein and guide the SAR study, we docked the most potent compound **21b** and reference compound HPOB into the human HDAC6 catalytic domain 2 (PDB code: 5EDU) using the Cdocker software. As shown in **Fig**. **5(a)**, **21b** fits perfectly into the hydrophobic channel of the binding pocket and exhibits a monodentate hydroxamate-Zn^{2+} coordination with a $Zn^{2+}\cdots O$ separation of 1.96 Å. While the hydroxamate C=O group forms a hydrogen bond with the Zn^{2+}-bound water molecule ($O\cdots H$ separation = 2.10 Å). This unusual zinc-binding mode has been confirmed in many crystal structures of zHDAC6 complexed with the sHDAC6is[32]. A similar orientation of the phenylhydroxamic acid group of HPOB was found (**Fig. 5b**). It was reported that the interaction between inhibitor and the L1 loop was important for HDAC6 selectivity[33]. As illustrated in **Fig**. **5(a)**, the nitrogen atom of indolyl group forms a hydrogen bond with a water molecule which interacts with the carboxyl residue of Asp497. And this probably leads to the gap of enzymatic activities between **21b** and **11b** which bears a phenyl as the capping group.

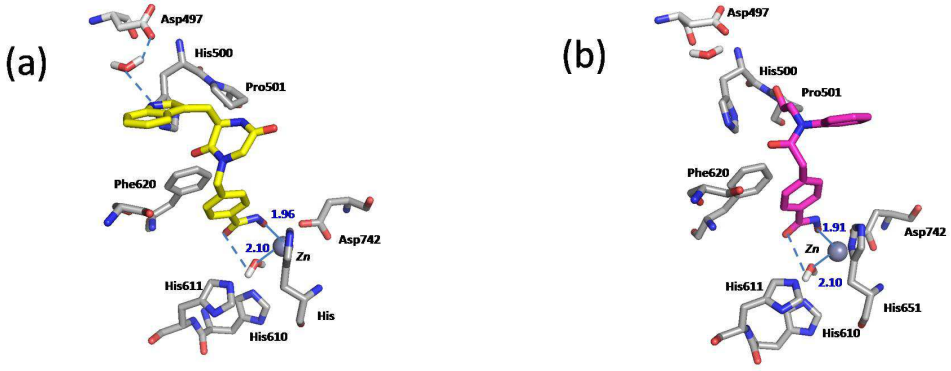

Fig 5(a). Docking model of **21b** (yellow) in complex with hHDAC6. Metal coordination and hydrogen bond interactions were indicated by solid and dashed blue lines, respectively. Distances between the hydroxamate and zinc ion/water are given in Å. (b) Docking model of HPOB (magenta) in complex with hHDAC6.The key residues were labeled in white. Zinc ion was labeled in brown. For clarity, all hydrogen atoms were hidden except water molecule.

To rationalize the selectivity of **21b** over other HDACs, especially the class I isoforms, we also performed docking studies using the solved crystal structures of hHDAC1 (PDB code: 5ICN) and hHDAC8 (PDB code:

1W22). As show in **Fig**. **6(a)**, the phenylhydroxamic acid group of **21b** is not able to comfortably coordinate to the catalytic zinc ion at the bottom of the narrow and deep binding pocket in hHDAC1. The distances between the hydroxamate group and the zinc ion are obviously larger than those in zHDAC6. In the case of hHDAC8, the interaction of indolyl and DKP scaffold with the pocket rim is unfavorable. Besides, the crowed space in hHDAC8 surface formed by shorter loop makes **21b** in an awkward spatial conformation (**Fig**. **6b**). Thus, these results reveal the structural basis for the HDAC6 selectivity of the DKP analogues.

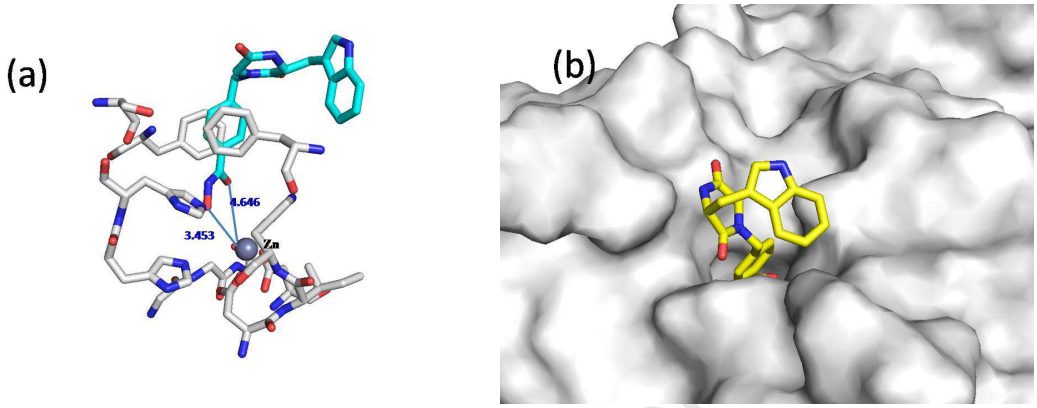

Fig 6. (a) The binding mode of **21b** (green) in complex with hHDAC1. Metal coordination interactions were indicated by solid blue lines. Distances between the hydroxamate and zinc ion are given in Å. (b) The binding mode of **21b** (yellow) in complex with hHDAC8. The key residues were labeled in white. Zinc ion was labeled in brown. For clarity, all hydrogen atoms were hidden.

2.5 *Antiproliferative activities of representative compounds*

Representative compounds **21b** and **18a** were selected for antiproliferative screening against a set of 59 solid or hematological tumor cell lines by NCI (termed NCI-60). The human tumor cell lines of the NCI-60 come from different tissue origins including blood, lung, colon, central nervous system (CNS), melanoma, ovary, kidney, prostate and breast. Concretely, compounds were screened at 10 μM concertration, and the growth percents (GP) of the cells were calculated. As displayed in **Table 3**, the most potent compound **21b** dramatically showed no or weak antiproliferative activities against most cell lines (GP values > 80%) except HCT116 cell line (colon cancer) with the GP value of 54.88%. Despite weaker HDAC6 and HDAC1 inhibitions than **21b**, **18a** seemed to have overall superior activities against almost all the tumor cell lines. The probable cause of this division might be the better lipophicity that made **18a** penetrate the cell membrane more easily. However, the antiproliferative effects of **18a** were also not remarkable. Among these, Leukemia cells such as RPMI-8226 and SR were more sensitive to **18a**, with GP values of 58.59% and 63.55% respectively.

Table 3

In vitro antiproliferative screening against 60 cell lines of **21b** and **18a** (Growth percents[a] at 10 μM concentration).

Origin of cancer	Cell line	**21b**	**18a**	Origin of cancer	Cell line	**21b**	**18a**
Leukemia	CCRF-CEM	102.54	71.99		M14	94.21	90.38
	HL60 (TB)	126.17	101.78		MDA-MB-435	101.95	91.28
	K562	100.38	76.44		SK-MEL-2	112.53	99.38
	MOLT-4	86.85	76.65		SK-MEL-28	110.47	95.44
	RPMI-8226	103.80	**58.59**		SK-MEL-5	108.43	96.65
	SR	114.92	**63.55**		UACC-257	96.14	69.30
Non-Small Cell	A549/ATCC	96.58	95.08		UACC-62	95.45	87.52
Lung Cancer	EKVX	106.25	88.17	Ovarian Cancer	IGROV1	101.25	88.98

	HOP-62	102.20	87.83		OVCAR-3	104.28	79.72
	HOP-92	103.95	101.66		OVCAR-4	/	66.45
	NCI-H226	97.56	/		OVCAR-5	106.97	97.79
	NCI-H23	101.09	86.72		OVCAR-8	94.84	74.97
	NCI-H322M	99.12	89.50		NCI/ADR-RES	104.22	94.55
	NCI-H460	104.28	81.58		SK-OV-3	96.53	90.43
	NCI-H522	96.68	**69.76**	Renal Cancer	786-0	83.05	94.75
Colon Cancer	COLO 205	120.39	89.18		A498	84.95	**67.39**
	HCC-2998	103.46	85.88		ACHN	104.01	90.63
	HCT-116	**54.88**	84.14		CAKI-1	93.77	96.45
	HCT-15	103.26	74.31		RXF 393	104.86	86.04
	HT29	104.25	87.86		SN12C	100.35	96.57
	KM12	102.18	86.93		TK-10	103.02	88.12
	SW-620	103.39	94.06		UO-31	91.06	**69.49**
CNS Cancer	SF-268	99.26	96.51	Prostate Cancer	PC-3	97.49	76.55
	SF-295	105.35	100.46		DU-145	106.54	86.95
	SF-539	107.20	87.34	Breast Cancer	MCF7	96.67	82.86
	SNB-19	96.85	85.43		MDA-MB-231/ATCC	107.24	95.19
	SNB-75	94.54	**69.38**		HS 578T	103.99	82.00
	U251	96.73	81.32		BT-549	98.22	102.82
Melanoma	LOX IMVI	106.48	93.21		T-47D	87.29	**69.11**
	MALME-3M	94.64	77.06		MDA-MB-468	106.87	79.92

[a]The values of cells growth percents were provided by NCI-60 program.

Based on the results in **Table 3**, compounds **11b**, **18a**, **18b**, **18d** and **21b** were selected for the IC_{50} evaluation against two multiple myeloma cells RPMI-8226 and U266, using the clinical sHDAC6i ACY-1215 and SAHA as the positive compounds (**Table 4**). In comparison of ACY-1215, U266 cell was more sensitive to all five compounds which had IC_{50} values in double-digit micromole range. Besides, **18a**, **18b** and **18d** exhibited antiproliferative activities against RPMI-8226 cell comparable to that of ACY-1215 with IC_{50} values of 11.650 μM, 12.130 μM and 13.420 μM, respectively. However, **11b** and **21b**, with better effects on HDAC6 inhibition, did not show matched antiproliferative activities, and this might be due to their poor hydrophobicity. Compared to sHDAC6is including DKPs and ACY-1215, nonselective SAHA had an obviously better activity. In addition, all the DKP derivatives showed no influence on normal bone marrow cell HS-5.

Table 4

Growth inhibition (IC_{50}, μM) of **18a**, **18b**, **21b** and reference compounds ACY-1215, SAHA against RPMI-8226 and U266 cell lines.

Compound	RPMI-8226	U266	HS-5
11b	54.370± 3.055	86.340± 8.900	> 100
18a	11.650± 0.845	25.882± 1.236	> 100
18b	12.130± 1.220	23.370± 2.105	> 100
18d	13.420± 0.860	23.100± 2.430	> 100
21b	33.183± 2.140	43.233± 5.474	> 100
ACY-1215	9.260± 0.842	> 100	/

SAHA	0.684± 0.083	0.590± 0.012	/

A lot of researches had reported the combined treatment of HDAC6 inhibitor and anticancer agents in various tumors. In this research, combination of **18a** and adriamycin was performed to determine whether the synergistic antiproliferative effect could occur in solid tumor non-small cell lung cancer cell A549. As shown in **Table 5**, compound **18a** and adriamycin exhibited significant antiproliferative influence on A549 cell with combination index (CI_{50}) of 0.676. This finding suggested that combined DKP derivative **18a** and adriamycin warranted attention for cancer treatment.

Table 5

Combined cytotoxic effect of **18a** and adriamycin on A549 cell line.

Compound	IC_{50} for individual use	IC_{50} for combination
18a	100 μM	8.17 μM
adriamycin	255 nM	152 nM
CI_{50}[a]	0.676	

[a]The calculation of CI_{50} value was as shown in experimental section.

2.6 *Microsomal stability study*

Preliminary stability evaluation of compounds **18a** and **18b** in human liver microsome was performed to determinate half-life ($T_{1/2}$). As shown in **Table 6**, the elimination $T_{1/2}$ values of **18a** and **18b** were 9.7 h and 10.1 h in HLM, better than that of ACY-1215 (7.5 h).

Table 6

In vitro stabilities of compounds **18a**, **18b** and ACY-1215 toward HLM.

Compound	HLM Concentration	Substrate Concentration	$T_{1/2}$
18a	0.8 mg/mL	0.5 μM	9.7 h
18b	0.8 mg/mL	0.5 μM	10.1 h
ACY-1215	0.8 mg/mL	0.5 μM	7.5 h

3. Conclusion

In summary, we designed a series of novel HDAC6 inhibitors bearing natural DKP scaffold and developed a convenient synthesis to prepare them. Most of these derivatives exhibited distinct inhibitory activities and selectivity toward HDAC6. The most potent compound **21b** showed an IC_{50} value of 0.73 nM against HDAC6 and 10941-fold selectivity over HDAC1. Although weaker enzymatic activity was observed for **18a**, it performed better than **21b** in the NCI antitumor screening toward 59 cell lines. Compared to ACY-1215, **18a**, **18b** and **18d** displayed superior or comparable antiproliferative activities against two multiple myeloma cells with IC_{50} values in the low micromolar range. Moreover, the combination of **18a** and adriamycin was more potent than either compound alone. Besides, **18a** and **18b** also had favorable metabolic stability in HLM. Our results demonstrated that these DKP derivatives deserved further structural modifications and in vivo pharmacological evaluation.

4. Experimental section

4.1 Chemistry

All reagents and solvents were reagent grade or were purified by standard methords before used in the lab.

Isolation and purification of the compounds were performed by flash column chromatography on silica gel 60 (230-400 mesh). Analytical thin-layer chromatography (TLC) was conducted on fluka TLC plates (silica gel 60 F254, aluminum foil). The structures of synthesized compounds were characterized by ^{1}H NMR, ^{13}C NMR and MS. The structural information and detailed synthetic process for the intermediates and target compounds are shown in this section. Melting points were measured using an X-4 melting-point apparatus with a microscope (Beijing Tech Instrument) and were not corrected. ^{1}H and ^{13}C NMR spectra were recorded in DMSO-d_6 by a 500 MHz spectrometer: chemical shifts (δ) are given in parts per million, coupling constants (J) in Hz. MS were determined by a Nicolet 2000 FT-IR mass spectrometer and MAT-212 mass spectrometer. All of the target compounds were examined by HPLC, and the purity of every case was ≥ 95%. Reverse-phase HPLC was performed on an Agilent Technologies 1260 Infinity, which was equipped with a C18 column (Agilent Zorbax SB-C18, 5 μM, 4.6 mM × 150 mM). Mobile phase A was acetonitrile, and mobile phase B was water.

4.1.1 General procedure for the synthesis of DKP scaffolds ***8a-b***, ***12***, ***17a-e*** *and* ***20a-b***.

Various amino acid esters (0.1 mol) and triethylamine (69.3 mL, 0.5 mol) were added in 250 mL anhydrous acetonitrile at 0 °C. Then resulting mixture was stirred for 10 minutes. 2-chloroacetyl chloride (8 mL, 0.1 mol) was added to the reaction solution and the resulting mixture was stirred for additional 1 hour at 0 °C, and treated with methyl 4-(aminomethyl)benzoate hydrochloride (20.17 g, 0.1 mol). The reaction mixture was heated to reflux for 6 h, then concentrated in vacuo to remove needless triethylamine. To the mixture was added 10% silica gel (5.5 g) and 200 mL additional acetonitrile, then the mixture was refluxed overnight and monitored end by TLC. The product was obtained as a white solid by chromatography on a silica gel column.

*4.1.1.1 Methyl (S)-4-((3-benzyl-2, 5-dioxopiperazin-1-yl)methyl)benzoate (****8a****).* 81.7% isolated yield; white solid; MS (ESI, m/z): 375.4 $[M+Na]^+$; Mp: 118-120 °C. ^{1}H-NMR (500 MHz, DMSO-d_6) δ*:* 8.40 (s, 1H), 7.78 (d, J = 8.22 Hz, 2H), 7.56 (d, J = 7.9 Hz, 1H), 7.39 (d, J = 8.1 Hz, 1H), 7.11 (t, J = 7.2 Hz, 1H), 7.06 (s, 1 H), 7.00 (t, J = 7.1 Hz, 1H), 6.96 (d, J = 8.1 Hz, 2H), 4.44 (d, J = 15.2 Hz, 1H), 4.28 (d, J = 15.2 Hz 2H), 3.87 (s, 3H), 3.50-3.36 (m, 2H), 3.07 (dd, J_1 = 14.4 Hz, J_2 = 4.1 Hz, 1H), 2.75 (t, J = 13.6 Hz, 1H).

*4.1.1.2 Methyl (R)-4-((3-benzyl-2, 5-dioxopiperazin-1-yl)methyl)benzoate (****8b****).* 85.6% isolated yield; white solid; MS (ESI, m/z): 375.4 $[M+Na]^+$; Mp: 119-121°C. ^{1}H-NMR (500 MHz, DMSO-d_6) δ*:* 8.40 (s, 1H), 7.92 (d, J = 8.2 Hz, 2H), 7.27 (d, J = 8.2 Hz, 2H), 7.23 (d, J = 7.2 Hz, 1H), 7.16 (t, J = 7.4 Hz, 2H), 7.10 (d, J = 7.1 Hz, 2H), 4.67 (d, J = 14.9 Hz, 1H), 4.29 (d, J = 15.0 Hz, 2H), 3.89 (s, 3H), 3.54 (d, J = 17.2 Hz, 1H), 3.18 (dd, J_1 = 13.5 Hz, J_2 = 3.8 Hz, 1H), 2.93 (dd, J_1 = 13.5 Hz, J_2 = 4.7 Hz, 1H), 2.74 (t, J = 17.3 Hz, 1H).

*4.1.1.3 Methyl (S)-3-((3-benzyl-2, 5-dioxopiperazin-1-yl)methyl)benzoate (****12****).* 92.3% yield, white solid. MS (ESI, m/z): 375.4 $[M+Na]^+$; Mp: 115-117 °C. ^{1}H-NMR (500 MHz, DMSO-d_6) δ*:* 8.26 (s, 1H), 7.96 (d, J = 8.0 Hz, 2H), 7.52 (s, 1H), 7.38 (s, 1H), 7.19 (s, 1H), 7.14 (t, J = 7.3 Hz, 2H), 7.12 (d, J = 7.5 Hz, 2H), 4.92 (d, J = 13.8 Hz, 1H), 4.46 (d, J = 15.2 Hz, 2H), 3.89 (s, 3H), 3.55 (d, J = 17.9 Hz, 1H), 3.19 (dd, J_1 = 13.1 Hz, J_2 = 3.8 Hz, 1H), 2.92 (dd, J_1 = 12.8 Hz, J_2 = 4.9 Hz, 1H), 2.75 (t, J = 17.2 Hz, 1H).

*4.1.1.4 methyl (R)-4-((3,4-dibenzyl-2,5-dioxopiperazin-1-yl)methyl)benzoate (****17a****)* 66.5% yield, white solid. MS (ESI, m/z): 443.5 $[M+H]^+$; Mp: 165-167 °C. ^{1}H-NMR (500 MHz, DMSO-d_6) δ: ^{1}H-NMR (500 MHz, DMSO-d_6) δ: 7.99 (s, 1H), 7.97 (s, 1H), 7.39 (dd, J_1 = 15.1, J_2 = 7.8 Hz, 4H), 7.33 (d, J = 7.8 Hz, 3H), 7.20 (d, J = 7.4 Hz, 1H), 7.05 (t, J = 7.6 Hz, 2H), 6.97 (d, J = 7.3 Hz, 2H), 5.17 (d, J = 14.9 Hz, 1H), 4.71 (d, J = 14.6 Hz, 1H), 4.25 (d, J = 14.5 Hz, 1H), 4.16 (d, J = 7.2 Hz, 1H), 3.90 (s, 3H), 3.61 (d, J = 17.1 Hz, 1H), 3.13-3.02 (m, 2H), 2.48 (d, J = 17.1

Hz, 2H).

4.1.1.5 Methyl (R)-4-((3-benzyl-4-(2-chlorobenzyl)-2, 5-dioxopiperazin-1-yl)methyl)benzoate ***(17b)*** 78.1% yield, white solid. MS (ESI, m/z): 477.2 $[M+H]^+$; Mp: 178-180 °C. ^{1}H-NMR (500 MHz, DMSO-d_6) δ: 7.96 (s, 1H), 7.80 (d, J = 7.8 Hz, 2H), 7.34 (t, J = 8.4 Hz, 3H), 7.20 (t, J = 7.0 Hz, 1H), 7.11 (t, J = 7.3 Hz, 2H), 7.02 (d, J = 7.2 Hz, 2H), 5.22 (d, J = 15.5 Hz, 1H), 4.65 (d, J = 14.5 Hz, 1H), 4.31 (d, J = 14.6 Hz, 1H), 4.25-4.10 (m, 2H), 3.89 (s, 3H), 3.63 (s, 1H), 3.27 (dd, J_1 = 13.5 Hz, J_2 = 4.4 Hz, 1H), 3.16-3.06 (m, 1H), 2.56 (d, J = 17.2 Hz, 1H).

4.1.1.6 Methyl (R)-4-((3-benzyl-4-(4-chlorobenzyl)-2, 5-dioxopiperazin-1-yl)methyl)benzoate ***(17c)*** 85.2% yield, white solid. MS (ESI, m/z): 477.2 $[M+H]^+$; Mp: 196-198 °C. ^{1}H-NMR (500 MHz, DMSO-d_6) δ: 7.97 (s, 1H), 7.80 (d, J = 7.7 Hz, 2H), 7.43 (s, 1H), 7.37 (d, J = 7.5 Hz, 2H), 7.30 (d, J = 7.7 Hz, 2H), 7.19 (t, J = 6.9 Hz, 1H), 7.04 (t, J = 7.1 Hz, 2H), 6.96 (d, J = 7.1 Hz, 2H), 5.16 (d, J = 15.0 Hz, 1H), 4.66 (d, J = 14.4 Hz, 1H), 4.38-4.00 (m, 3H), 3.90 (s, 3H), 3.57 (d, J = 17.1 Hz, 1H), 3.27 (d, J = 9.8 Hz, 1H), 3.11 (d, J = 11.9 Hz, 1H), 2.43 (d, J = 16.9 Hz, 1H).

4.1.1.7 Methyl (R)-4-((3-benzyl-4-(3-chlorobenzyl)-2,5-dioxopiperazin-1-yl)methyl)benzoate ***(17d)*** 81.6% yield, white solid. MS (ESI, m/z): 477.2 $[M+H]^+$; Mp: 183-185 °C. ^{1}H-NMR (500 MHz, DMSO-d_6) δ: 7.96 (s, 1H), 7.81 (d, J = 7.8 Hz, 2H), 7.41 (t, J = 6.9 Hz, 2H), 7.32 (s, 2H), 7.20 (t, J = 7.1 Hz, 1H), 7.05 (t, J = 7.3 Hz, 2H), 6.95 (d, J = 7.3 Hz, 2H), 5.14 (d, J = 15.1 Hz, 1H), 4.67 (d, J = 14.5 Hz, 1H), 4.24 (dd, J_1 = 27.0 Hz, J_2 = 11.4 Hz, 3H), 3.90 (s, 3H), 3.59 (d, J = 17.1 Hz, 1H), 3.26 (dd, J_1 = 13.4 Hz, J_2 = 4.1 Hz, 1H), 3.11 (d, J = 11.2 Hz, 1H), 2.46 (d, J = 17.2 Hz, 1H).

4.1.1.8 Methyl (R)-4-((3-benzyl-4-(3-methoxybenzyl)-2, 5-dioxopiperazin-1-yl)methyl)benzoate ***(17e)*** 82.0% yield, white solid. MS (ESI, m/z): 495.2 $[M+Na]^+$; Mp: 176-178 °C. ^{1}H-NMR (500 MHz, DMSO-d_6) δ: 7.97 (s, 2H), 7.80 (d, J = 7.7 Hz, 2H), 7.31 (d, J = 7.5 Hz, 2H), 7.20 (t, J = 7.0 Hz, 1H), 7.06 (t, J = 7.2 Hz, 2H), 6.98 (d, J = 7.2 Hz, 2H), 6.90 (s, 2H), 5.19 (d, J = 15.0 Hz, 1H), 4.65 (d, J = 14.5 Hz, 1H), 4.25 (d, J = 14.5 Hz, 1H), 4.21 (s, 1H), 4.12 (d, J = 14.9 Hz, 1H), 3.91 (s, 3H), 3.76 (s, 3H), 3.61 (s, 1H), 3.34-3.20 (m, 1H), 3.10 (d, J = 11.1 Hz, 1H), 2.49 (d, J = 17.1 Hz, 1H).

4.1.1.9 Methyl (S)-4-((3-((1H-indol-3-yl)methyl)-2, 5-dioxopiperazin-1-yl)methyl)benzoate ***(20a)*** 89.0% yield, white solid. MS (ESI, m/z): 392.2 $[M+H]^+$; Mp: 156-158 °C. ^{1}H-NMR (500 MHz, DMSO-d_6) δ: 9.06 (s, 1H), 8.41 (d, J = 2.3 Hz, 1H), 7.61 (d, J = 8.2 Hz, 2H), 7.53 (s, 1H), 7.40 (d, J = 8.1 Hz, 1H), 7.10 (t, J = 7.5 Hz, 1H), 7.06 (d, J = 2.1 Hz, 1H), 7.00 (t, J = 7.4 Hz, 1H), 6.92 (d, J = 8.1 Hz, 2H), 4.31 (d, J = 3.6 Hz, 2H), 4.29-4.26 (m, 1H), 3.91 (s, 3H), 3.37 (s, 1H), 3.36 (d, J = 6.7 Hz, 1H), 3.08 (dd, J_1 = 14.4 Hz, J_2 = 4.3 Hz, 1H), 2.73 (d, J = 17.1 Hz, 1H).

4.1.1.10 Methyl (R)-4-((3-((1H-indol-3-yl)methyl)-2, 5-dioxopiperazin-1-yl)methyl)benzoate ***(20b)*** 90.3% yield, white solid. MS (ESI, m/z): 392.2 $[M+H]^+$; Mp: 160-162 °C. ^{1}H-NMR (500 MHz, DMSO-d_6) δ: 9.04 (s, 1H), 8.37 (s, 1H), 7.57 (dd, J_1= 14.2, J_2 = 7.9 Hz, 3H), 7.41 (d, J = 8.1 Hz, 1H), 7.10 (t, J = 7.5 Hz, 1H), 7.05 (s, 1H), 7.02 (t, J = 7.4 Hz, 1H), 6.95 (d, J = 7.8 Hz, 2H), 4.30 (d, J = 8.5 Hz, 2H), 4.28 (s, 1H), 3.43-3.38 (m, 1H), 3.91 (s, 3H), 3.20 (d, J = 4.8 Hz, 1H), 3.07 (dd, J_1= 14.3, J_2 = 3.7 Hz, 1H), 2.74 (d, J = 17.2 Hz, 1H).

4.1.2 General procedure for the preparation of intermediates ***14a-c****.*

To a mixture of **8a** (35.2 mg, 0.1mmol) in anhydrous THF (25 mL) was slowly added NaH (4.4 mg, 0.11

mmol) in batches at 0 °C. After 5 min, halohydrocarbon (0.1 mmol) was added. Then, the mixture was heated to reflux for 6 h. The reaction was monitored by TLC until the maximum conversion. Methanol was added to quench the reaction, then the mixture was poured into water (30 mL) and extracted with EtOAc (3×30 mL). The combined organic extracts were washed with brine (2×30 mL), dried over anhydrous Na_2SO_4 and concentrated in vacuo. The product was obtained by chromatography on a silica gel column.

*4.1.2.1 Methyl 4-((3-benzyl-4-methyl-2, 5-dioxopiperazin-1-yl)methyl)benzoate (**14a**)* 45.3% yield, white solid. MS (ESI, m/z): 367.2 $[M+H]^+$; Mp: 120-122 °C. ^{1}H-NMR (500 MHz, DMSO-d_6) δ: 7.96 (d, J = 7.0 Hz, 2H), 7.36 (d, J = 7.1 Hz, 2H), 7.20 (d, J = 6.8 Hz, 1H), 7.07 (t, J = 6.7 Hz, 2H), 6.97 (d, J = 6.8 Hz, 2H), 4.58 (d, J = 14.6 Hz, 1H), 4.41 (s, 1H), 4.33 (d, J = 14.5 Hz, 1H), 3.89 (s, 3H), 3.47 (d, J = 17.1 Hz, 1H), 3.18 (d, J = 12.9 Hz, 1H), 3.10 (d, J = 12.9 Hz, 1H), 2.96 (s, 3H), 2.35 (d, J = 17.1 Hz, 1H).

*4.1.2.2 Methyl 4-((4-allyl-3-benzyl-2, 5-dioxopiperazin-1-yl)methyl)benzoate (**14b**)* 61.0% yield, white solid. MS (ESI, m/z): 443.2 $[M+H]^+$; Mp: 173-175 °C. ^{1}H-NMR (500 MHz, DMSO-d_6) δ: 7.97 (d, J = 7.2 Hz, 2H), 7.38 (d, J = 7.0 Hz, 2H), 7.20 (d, J = 6.2 Hz, 1H), 7.05 (d, J = 6.0 Hz, 2H), 6.98 (d, J = 6.0 Hz, 2H), 5.84 (d, J = 5.5 Hz, 1H), 5.32-5.13 (m, 2H), 4.66 (d, J = 14.5 Hz, 1H), 4.52 (d, J = 15.1 Hz, 1H), 4.29 (d, J = 20.0 Hz, 2H), 3.89 (s, 3H), 3.59 (dd, J_1 = 14.5 Hz, J_2 = 5.9 Hz, 1H), 3.53 (d, J = 17.1 Hz, 1H), 3.14 (dd, J_1 = 59.2 Hz, J_2 = 13.0 Hz, 2H), 2.42 (d, J = 17.0 Hz, 1H).

*4.1.2.3 Methyl 4-((3,4-dibenzyl-2,5-dioxopiperazin-1-yl)methyl)benzoate (**14c**)* 58.0% yield, white solid. MS (ESI, m/z): 393.2 $[M+H]^+$; Mp: 154-156 °C. ^{1}H-NMR (500 MHz, DMSO-d_6) δ: 7.98 (d, J = 7.0 Hz, 2H), 7.49-7.27 (m, 7H), 7.19 (d, J = 6.4 Hz, 1H), 7.04 (s, 2H), 6.96 (d, J = 6.0 Hz, 2H), 5.17 (d, J = 15.1 Hz, 1H), 4.72 (d, J = 14.4 Hz, 1H), 4.24 (d, J = 14.5 Hz, 1H), 4.14 (d, J = 16.2 Hz, 2H), 3.90 (s, 3H), 3.61 (d, J = 17.0 Hz, 1H), 3.26 (d, J = 10.4 Hz, 1H), 3.07 (d, J = 13.0 Hz, 1H), 2.46 (d, J = 17.0 Hz, 1H).

*4.1.3 General procedure for the preparation of intermediates **16a-e**.*

To a solution of *D*-phenylalanine methyl ester hydrochloride (21.6 mg, 0.1 mmol) in MeOH (15 mL) was added various aromatic aldehydes (0.1 mmol). The resulting mixture was stirred vigorously at room temperature for 30 min. After confirmation of reaction completion by TLC, $NaBH_3CN$ was added slowly at 0 °C. The mixture was stirred at room temperature for 12 h. After removal of the solvent, H_2O was added to dissolve inorganic salt, and the mixture was extracted with EtOAc (3×20 mL). The organic layers were combined, washed with brine, and dried by anhydrous $MgSO_4$. The solvent was removed in vacuo, and the residue was purified by column chromatography.

*4.1.3.1 Methyl benzyl-D-phenylalaninate (**16a**)*

41.0% yield, white solid, MS (ESI, m/z): 270.3 $[M+H]^+$. ^{1}H-NMR (500 MHz, DMSO-d_6) δ: 7.48-7.43 (1H, m), 7.41 (1H, m), 7.30 (3H, t, J = 7.2 Hz), 7.28-7.22 (3H, m), 7.20 (2H, m), 3.77 (1H, t, J = 16.4 Hz), 3.66-3.59 (2H, m), 3.59 (3H, s), 3.51-3.42 (1H, m), 3.01-2.84 (2H, m).

*4.1.3.2 Methyl (2-chlorobenzyl)-D-phenylalaninate (**16b**)*

32.5% yield, white solid, MS (ESI, m/z): 303.2 $[M+H]^+$. ^{1}H-NMR (500 MHz, DMSO-d_6) δ: 7.15-7.48 (m, 9H), 3.69 (d, J = 13.5 Hz, 1H), 3.64 (d, J = 13.5 Hz, 1H), 3.55 (s, 3H), 3.52 (d, J = 6.5 Hz, 1H), 3.07 (d, J = 6.2 Hz, 2H), 2.44 (s, 1H).

*4.1.3.3 Methyl (4-chlorobenzyl)-D-phenylalaninate (**16c**)*

34.1% yield, white solid, MS (ESI, m/z): 303.2 $[M+H]^+$. ^{1}H-NMR (500 MHz, DMSO-d_6) δ: 7.63-7.49 (m, 4H), 7.27-7.15 (m, 5H), 3.79 (d, J = 12.9 Hz, 1H), 3.63 (d, J = 13.7 Hz, 1H), 3.56 (s, 3H), 3.45 (d, J = 6.6 Hz, 1H), 3.17 (d, J = 6.6 Hz, 2H), 2.44 (s, 1H).

*4.1.3.4 Methyl (3-chlorobenzyl)-D-phenylalaninate (**16d**)*

42.7% yield, white solid, MS (ESI, m/z): 303.2 $[M+H]^+$. ^{1}H-NMR (500 MHz, DMSO-d_6) δ: 7.16-7.60 (m, 9H), 3.80 (d, J = 13.7 Hz, 1H), 3.61 (d, J = 13.9 Hz, 1H), 3.53 (s, 3H), 3.52 (d, J = 6.5 Hz, 1H), 3.07 (d, J = 6.4 Hz, 2H), 2.48 (s, 1H).

*4.1.3.5 Methyl (3-methoxybenzyl)-D-phenylalaninate (**16e**)*

45.8% yield, white solid, MS (ESI, m/z): 300.2 $[M+H]^+$. ^{1}H-NMR (500 MHz, DMSO-d_6) δ: 7.35-7.14 (m, 7H), 6.90 (d, J = 8.8 Hz, 2H), 3.78 (d, J = 13.6 Hz, 1H), 3.64 (d, J = 13.4 Hz, 1H), 3.53 (s, 3H), 3.52 (d, J = 6.7 Hz, 1H), 3.02 (d, J = 6.6 Hz, 2H), 2.35 (s, 1H).

4.1.4 General procedure for the hydrolysis of esters to yield various acids

To a solution of various esters (1 mmol) in MeOH and H_2O (10 mL, v/v = 1: 1) was added lithium hydroxide (95.8 mg, 4 mmol) at 0 °C. Then, the mixture was allowed to stir at room temperature. The reaction was monitored by TLC until the maximum conversion. After neutralized with acetic acid, the formed precipitate was collected by filtration, washed with water, and dried in vacuo to give the title compounds.

*4.1.4.1 (S)-4-((3-benzyl-2, 5-dioxopiperazin-1-yl)methyl)benzoic acid (**9a**)* 78.2% yield, white solid, MS (ESI, m/z): 339.1 $[M+H]^+$. ^{1}H-NMR (500 MHz, DMSO-d_6) *δ:* 12.12 (s, 1H), 8.41 (s, 1H), 7.77 (d, J = 8.5 Hz, 2H), 7.58 (d, J = 7.2 Hz, 1H), 7.40 (d, J = 8.0 Hz, 1H), 7.20 (s, 1H), 7.09 (s, 1 H), 7.03 (t, J = 7.1 Hz, 1H), 6.70 (d, J = 8.1 Hz, 2H), 4.44 (d, J = 15.2 Hz, 1H), 4.28 (d, J = 15.2 Hz 2H), 3.52-3.37 (m, 2H), 3.08 (dd, J_1 = 14.2 Hz, J_2 = 4.4 Hz, 1H), 2.79 (m, 1H).

*4.1.4.2 (R)-4-((3-benzyl-2,5-dioxopiperazin-1-yl)methyl)benzoic acid (**9b**)* 69.3% yield, white solid, MS (ESI, m/z): 339.1 $[M+H]^+$. ^{1}H-NMR (500 MHz, DMSO-d_6) *δ:* 12.04 (s, 1H), 8.41 (s, 1H), 7.92 (d, J = 8.3 Hz, 2H), 7.28 (d, J = 7.9 Hz, 2H), 7.21 (s, 1H), 7.17 (t, J = 7.5 Hz, 2H), 7.10 (d, J = 7.2 Hz, 2H), 4.69 (d, J = 15.1 Hz, 1H), 4.30 (d, J = 15.0 Hz, 2H), 3.58 (d, J = 17.1 Hz, 1H), 3.20 (dd, J_1 = 13.3 Hz, J_2 = 3.6 Hz, 1H), 2.96 (m, 1H), 2.75 (t, J = 17.2 Hz, 1H).

4.1.5 General procedure for the amidation of various acids with O-(tetrahydro-2H-pyran-2-yl)hydroxylamine

To a solution of acid (1 mmol) in DMF (10 mL) were added DIPEA (0.66 mL, 4 mmol), HATU (353.2 mg, 1.1 mmol) at 0 °C. After 30 min, *O*-(tetrahydro-2*H*-pyran-2-yl)hydroxylamine (117.2 mg, 1 mmol) were added. The mixture was stirred for 5 h. After completion of the reaction as monitored by TLC, the mixture was poured into water (30 mL) and extracted with EtOAc (3×30 mL). The combined organic extracts were washed with brine (2 × 30 mL), dried over anhydrous Na_2SO_4 and concentrated in vacuo. The product was obtained by chromatography on a silica gel column.

*4.1.5.1 4-(((S)-3-benzyl-2,5-dioxopiperazin-1-yl)methyl)-N-((tetrahydro-2H-pyran-2-yl)oxy)benzamide (**10a**)*

53.6% yield, white solid. Mp: 193-195 °C. ^{1}H-NMR (500 MHz, DMSO-d_6) δ: 9.01 (s, 1H), 8.40 (s, 1H), 7.72 (d, J = 8.02 Hz, 2H), 7.13-7.17 (m, 5H), 7.08 (d, J = 7.4 Hz, 2H), 5.70 (s, 1H), 4.63 (d, J = 14.5 Hz, 1H), 4.30 (d, J =

2.1 Hz, 1H), 4.21 (d, *J* = 14.3 Hz, 1H), 3.74-3.64 (m, 2H), 3.50 (d, *J* = 17.1 Hz, 1H), 3.17 (d, *J* = 3.9 Hz, 1H), 2.99-2.90 (m, 1H), 2.70 (d, *J* = 17.2 Hz, 1H), 1.82-1.79 (m, 2H), 1.74-1.56 (m, 4H).

*4.1.5.2 4-(((R)-3-benzyl-2,5-dioxopiperazin-1-yl)methyl)-N-((tetrahydro-2H-pyran-2-yl)oxy)benzamide (**10b**)* 43.7% yield, white solid. Mp: 201-203 °C. ^{1}H-NMR (500 MHz, DMSO-d_6) δ: 9.03 (s, 1H), 8.37 (s, 1H), 7.70 (d, *J* = 7.9 Hz, 2H), 7.28-7.13 (m, 5H), 7.08 (d, *J* = 7.1 Hz, 2H), 5.72 (s, 1H), 4.59 (d, *J* = 14.3 Hz, 1H), 4.30 (s, 1H), 4.25 (d, *J* = 14.5 Hz, 1H), 3.75-3.68 (m, 2H), 3.50 (d, *J* = 17.1 Hz, 1H), 3.19 (dd, J_1 = 13.2 Hz, J_2 = 3.5 Hz, 1H), 2.92-2.85 (m, 1H), 2.80-2.65 (m, 1H), 1.80-1.56 (m, 6H).

4.1.6 General procedure for deprotection of tetrahydro-2H-pyran to yield hydroxylamines

To a solution of compound (1 mmol) in methanol (10 mL) was added TsOH·H_2O (0.2 mmol), and the mixture was stirred at room temperature for overnight. After removal of volatiles, residues were purified by chromatography on a silica gel column.

*4.1.6.1 (S)-4-((3-benzyl-2, 5-dioxopiperazin-1-yl)methyl)-N-hydroxybenzamide (**11a**)* 73.5% yield, white solid. Mp: 226-128 °C. ^{1}H-NMR (500 MHz, DMSO-d_6) δ: 11.28 (s, 1H), 9.09 (s, 1H), 8.41 (s, 1H), 7.73 (d, *J* = 8.1 Hz, 2H), 7.16 (td, J_1 = 7.2, J_2 = 3.1 Hz, 5H), 7.09 (d, *J* = 7.2 Hz, 2H), 4.65 (d, *J* = 14.7 Hz, 1H), 4.31 (d, *J* = 2.2 Hz, 1H), 4.23 (d, *J* = 14.7 Hz, 1H), 3.51 (d, *J* = 17.2 Hz, 1H), 3.17 (d, *J* = 3.9 Hz, 1H), 2.98-2.90 (m, 1H), 2.70 (d, *J* = 17.2 Hz, 1H). ^{13}C-NMR (126 MHz, DMSO-d_6) δ: 166.00, 165.27, 145.98, 138.25, 136.03, 130.55, 128.57, 128.54, 127.46, 127.26, 126.01, 56.01, 49.08, 48.91, 48.67. $[\alpha]_D^{20}$ = −0.49 (1.22 mg/mL, MeOH). HR-MS (ESI, *m*/z): Calcd for: 354.1448. ($C_{19}H_{20}N_3O_4^+$, $[M+H]^+$). Found: 354.1449.

*4.1.6.2 (R)-4-((3-benzyl-2, 5-dioxopiperazin-1-yl)methyl)-N-hydroxybenzamide (**11b**)* 72.1% yield, white solid. Mp: 211-212 °C. **11b** (*R*-configuration) showed almost the same proton resonances as the enantiomer **11a** (*S*-configuration). In the lower field, nine proton signals indicated two groups of aryl protons resonance. Higher-field signals showed three pairs of methylene groups with coupling constants 14.7, 17.2 and 13.3 Hz. The proton signal of chiral C-3 on DKP skeleton is consistent with **11a**. ^{1}H-NMR (500 MHz, DMSO-d_6) δ: 11.23 (s, 1H), 9.04 (s, 1H), 8.36 (s, 1H), 7.71 (d, *J* = 8.1 Hz, 2H), 7.28-7.13 (m, 5H), 7.09 (d, *J* = 7.1 Hz, 2H), 4.64 (d, *J* = 14.7 Hz, 1H), 4.31 (m, 1H), 4.24 (d, *J* = 14.7 Hz, 1H), 3.52 (d, *J* = 17.2 Hz, 1H), 3.18 (dd, J_1 = 13.3 Hz, J_2 = 3.6 Hz, 1H), 2.99-2.88 (m, 1H), 2.80-2.68 (m, 1H). ^{13}C-NMR (126 MHz, DMSO-d_6) δ: 165.97, 165.27, 145.98, 139.37, 136.02, 130.55, 128.58, 128.55, 127.52, 127.27, 55.99, 48.92, 48.66. $[\alpha]_D^{25}$ = −0.47 (1.06 mg/mL, MeOH). HR-MS (ESI, *m*/z): Calcd for: 354.1448. ($C_{19}H_{20}N_3O_4^+$, $[M+H]^+$). Found: 354.1449.

*4.1.6.3 (S)-3-((3-benzyl-2, 5-dioxopiperazin-1-yl)methyl)-N-hydroxybenzamide (**13**)* 62.1% yield, white solid. Mp: 176-178 °C. ^{1}H-NMR (500 MHz, DMSO-d_6) δ: 11.32 (s, 1H), 9.12 (s, 1H), 8.40 (s, 1H), 7.71 (d, *J* = 7.0 Hz, 1H), 7.66 (s, 1H), 7.53 (d, *J* = 7.1 Hz, 2H), 7.41 (t, *J* = 7.1 Hz, 1H), 7.28 (d, *J* = 6.5 Hz, 1H), 7.15 (s, 1H), 7.10 (s, 1H), 7.06 (s, 1H), 4.61 (d, *J* = 14.4 Hz, 1H), 4.26 (d, *J* = 15.2 Hz, 2H), 3.50 (d, *J* = 17.2 Hz, 1H), 3.17 (d, *J* = 13.1 Hz, 1H), 2.93 (d, *J* = 13.4 Hz, 1H), 2.65 (d, *J* = 17.2 Hz, 1H). ^{13}C-NMR (126 MHz, DMSO-d_6) δ: 166.03, 165.37, 145.87, 138.32, 136.52, 135.93, 131.57, 130.50, 128.99, 128.60, 128.48, 127.68, 127.21, 126.48, 126.01, 55.99, 48.81. $[\alpha]_D^{25}$ = −0.67 (1.16 mg/mL, MeOH). HR-MS (ESI, *m*/z): Calcd for: 354.1448. ($C_{19}H_{20}N_3O_4^+$, $[M+H]^+$). Found: 354.1449.

*4.1.6.4 4-((3-benzyl-4-methyl-2, 5-dioxopiperazin-1-yl)methyl)-N-hydroxybenzamide (**15a**)* 83.3% isolated yield; white solid. Mp: 190-192 °C; ^{1}H-NMR (500 MHz, DMSO-d_6) δ: 11.26 (s, 1H), 9.07 (s, 1H), 7.75 (d, *J* = 8.1 Hz,

2H), 7.28 (d, *J* = 8.1 Hz, 2H), 7.20 (t, *J* = 7.4 Hz, 1H), 7.07 (t, *J* = 7.6 Hz, 2H), 6.96 (d, *J* = 7.3 Hz, 2H), 4.56 (d, *J* = 14.5 Hz, 1H), 4.40 (t, *J* = 4.1 Hz, 1H), 4.28 (d, *J* = 14.5 Hz, 1H), 3.45 (d, *J* = 17.0 Hz, 1H), 3.14 (m, 2H), 2.95 (s, 3H), 2.32 (d, *J* = 17.0 Hz, 1H). ^{13}C-NMR (126 MHz, DMSO-d_6) δ: 166.01, 163.98, 139.17, 135.58, 132.56, 130.15, 129.02, 128.67, 127.59, 127.52, 62.84, 48.68, 48.60, 36.63, 31.99. HR-MS (ESI, m/z): Calcd for: 368.16048. ($C_{20}H_{22}N_3O_4^+$, $[M+H]^+$). Found: 368.16068.

4.1.6.5 4-((4-allyl-3-benzyl-2, 5-dioxopiperazin-1-yl)methyl)-N-hydroxybenzamide ***(15b)*** 79.2% isolated yield; white solid. Mp: 194-195 °C**;** ^{1}H-NMR (500 MHz, DMSO-d_6) δ: 11.27 (s, 1H), 9.08 (s, 1H), 7.76 (d, *J* = 7.6 Hz, 2H), 7.30 (d, *J* = 7.7 Hz, 2H), 7.20 (t, *J* = 7.1 Hz, 1H), 7.06 (t, *J* = 7.2 Hz, 2H), 6.97 (d, *J* = 7.2 Hz, 2H), 5.95-5.74 (m, 1H), 5.35-5.17 (m, 2H), 4.62 (d, *J* = 14.4 Hz, 1H), 4.52 (d, *J* = 14.4 Hz, 1H), 4.25 (d, *J* = 13.8 Hz, 2H), 3.59 (dd, J_1 = 15.3 Hz, J_2 = 6.6 Hz, 1H), 3.51 (d, *J* = 17.0 Hz, 1H), 3.20 (dd, J_1 = 13.6, J_2 = 4.2 Hz, 1H), 3.09 (d, *J* = 13.0 Hz, 1H), 2.41 (d, *J* = 17.0 Hz, 1H). ^{13}C-NMR (126 MHz, DMSO-d_6) δ: 166.05, 164.42, 164.09, 139.22, 135.51, 133.12, 132.61, 130.28, 129.08, 128.67, 127.58, 118.67, 60.47, 48.80, 48.74, 45.91, 36.85. HR-MS (ESI, m/z): Calcd for 394.17613. ($C_{22}H_{24}N_3O_4^+$ $[M+H]^+$). Found 394.17633.

4.1.6.6 4-((3, 4-dibenzyl-2, 5-dioxopiperazin-1-yl)methyl)-N-hydroxybenzamide ***(15c)*** 91.2% isolated yield; white solid. Mp: 218-220 °C; ^{1}H-NMR (500 MHz, DMSO-d_6) δ: 11.27 (s, 1H), 9.08 (s, 1H), 7.98 (s, 1H), 7.77 (d, *J* = 8.2 Hz, 2H), 7.41 (t, *J* = 7.3 Hz, 2H), 7.34 (d, *J* = 2.0 Hz, 2H), 7.30 (d, *J* = 8.2 Hz, 2H), 7.20 (t, *J* = 7.4 Hz, 1H), 7.05 (t, *J* = 7.6 Hz, 2H), 6.96 (d, *J* = 7.2 Hz, 2H), 5.17 (d, *J* = 15.0 Hz, 1H), 4.67 (d, *J* = 14.4 Hz, 1H), 4.21 (d, *J* = 14.4 Hz, 1H), 4.18-4.14 (m, 2H), 4.13 (s, 1H), 3.59 (d, *J* = 17.1 Hz, 1H), 3.26 (dd, J_1 = 13.8 Hz, J_2 = 5.2 Hz, 1H), 3.08 (dd, J_1 = 13.8, J_2 = 3.7 Hz, 1H), 2.47 (d, *J* = 17.1 Hz, 1H). ^{13}C-NMR (126 MHz, DMSO-d_6) δ: 165.98, 164.59, 162.79, 139.17, 137.07, 135.49, 132.62, 130.28, 129.21, 129.10, 128.69, 128.52, 128.11, 127.60, 127.57, 60.61, 48.84, 48.80, 46.53, 36.76. HR-MS (ESI, m/z): Calcd for 444.19178. ($C_{26}H_{26}N_3O_4^+$ $[M+H]^+$). Found 444.19186.

4.1.6.7 (R)-4-((3, 4-dibenzyl-2, 5-dioxopiperazin-1-yl)methyl)-N-hydroxybenzamide ***(18a)*** 61.3% isolated yield; white solid. Mp: 220-222 °C; ^{1}H NMR (500 MHz, DMSO-d_6) δ: 11.27 (s, 1H), 9.07 (s, 1H), 7.77 (d, *J* = 7.9 Hz, 2H), 7.41 (t, *J* = 7.3 Hz, 2H), 7.33 (d, *J* = 7.1 Hz, 3H), 7.30 (d, *J* = 8.0 Hz, 2H), 7.20 (t, *J* = 7.1 Hz, 1H), 7.06 (t, *J* = 7.5 Hz, 2H), 6.96 (d, *J* = 7.5 Hz, 2H), 5.17 (d, *J* = 15.0 Hz, 1H), 4.67 (d, *J* = 14.5 Hz, 1H), 4.21 (d, *J* = 14.5 Hz, 1H), 4.16 (s, 2H), 4.13 (s, 1H), 3.59 (dd, J_1 = 17.1 Hz, J_1 = 9.0 Hz, 1H), 3.25 (d, *J* = 4.9 Hz, 1H), 3.13-3.02 (m, 1H), 2.47 (d, *J* = 16.9 Hz, 1H). ^{13}C-NMR (126 MHz, DMSO-d_6) δ: 165.99, 164.59, 162.80, 139.18, 137.06, 135.50, 132.63, 130.28, 130.00, 129.21, 129.09, 128.69, 128.52, 128.11, 127.60, 60.63, 48.85, 48.80, 46.55, 36.27. $[\alpha]_D^{25}$ = −2.02 (1.37 mg/mL, MeOH). HR-MS (ESI, m/z): Calcd for 444.19178. ($C_{26}H_{26}N_3O_4^+$ $[M+H]^+$). Found 444.19186.

4.1.6.8 (R)-4-((3-benzyl-4-(2-chlorobenzyl)-2, 5-dioxopiperazin-1-yl)methyl)-N-hydroxybenzamide ***(18b)*** 63.5% isolated yield; white solid. Mp: 225-227 °C; ^{1}H-NMR (500 MHz, DMSO-d_6) δ: 11.38 (s, 1H), 9.20 (s, 1H), 7.97 (s, 1H), 7.81 (d, *J* = 7.8 Hz, 2H), 7.33 (t, *J* = 8.4 Hz, 3H), 7.22 (t, *J* = 7.0 Hz, 1H), 7.10 (t, *J* = 7.3 Hz, 2H), 7.03 (d, *J* = 7.2 Hz, 2H), 5.23 (d, *J* = 15.5 Hz, 1H), 4.64 (d, *J* = 14.5 Hz, 1H), 4.32 (d, *J* = 14.5 Hz, 1H), 4.26-4.11 (m, 2H), 3.62 (s, 1H), 3.28 (dd, J_1 = 13.5 Hz, J_2 = 4.4 Hz, 1H), 3.18-3.08 (m, 1H), 2.57 (d, *J* = 17.2 Hz, 1H). ^{13}C-NMR (126 MHz, DMSO-d_6) δ: 165.99, 164.81, 162.88, 139.28, 135.38, 133.84, 133.15, 132.47, 130.30, 130.16, 129.97, 129.03, 128.97, 128.77, 127.95, 127.66, 127.60, 60.94, 48.82, 48.75, 44.94, 36.97. $[\alpha]_D^{25}$ = 3.46 (1.20 mg/mL, MeOH). HR-MS (ESI, m/z): Calcd for 478.15281. ($C_{26}H_{25}ClN_3O_4^+$$[M+H]^+$). Found 478.15289.

4.1.6.9 (R)-4-((3-benzyl-4-(4-chlorobenzyl)-2, 5-dioxopiperazin-1-yl)methyl)-N-hydroxybenzamide ***(18c)*** 58.0% isolated yield; white solid. Mp: 205-207 °C; ^{1}H-NMR (500 MHz, DMSO-d_6) δ: 11.38 (s, 1H), 9.20 (s, 1H), 7.97 (s,

1H), 7.80 (d, *J* = 7.7 Hz, 2H), 7.43 (s, 1H), 7.37 (d, *J* = 7.5 Hz, 2H), 7.31 (d, *J* = 7.7 Hz, 2H), 7.19 (t, *J* = 6.9 Hz, 1H), 7.05 (t, *J* = 7.1 Hz, 2H), 6.96 (d, *J* = 7.1 Hz, 2H), 5.15 (d, *J* = 15.0 Hz, 1H), 4.67 (d, *J* = 14.4 Hz, 1H), 4.38-4.00 (m, 3H), 3.57 (d, *J* = 17.1 Hz, 1H), 3.27 (d, *J* = 9.8 Hz, 1H), 3.11 (d, *J* = 11.9 Hz, 1H), 2.44 (d, *J* = 17.1 Hz, 1H). ^{13}C-NMR (126 MHz, DMSO-d_6) δ: 165.95, 164.68, 162.87, 139.19, 136.10, 135.34, 132.78, 132.46, 130.37, 130.25, 129.09, 128.68, 127.61, 60.77, 48.85, 48.78, 46.05, 36.79. $[\alpha]_D^{25}$ = 0.86 (1.14 mg/mL, MeOH). HR-MS (ESI, m/z): Calcd for 478.15281. ($C_{26}H_{25}ClN_3O_4^+$[M+H]$^+$). Found 478.15289.

4.1.6.10 (R)-4-((3-benzyl-4-(3-chlorobenzyl)-2, 5-dioxopiperazin-1-yl)methyl)-N-hydroxybenzamide ***(18d)*** 78.2% isolated yield; white solid. Mp: 231-233 °C; ^{1}H-NMR (500 MHz, DMSO-d_6) δ: 11.36 (s, 1H), 9.17 (s, 1H), 7.97 (s, 2H), 7.80 (d, *J* = 7.8 Hz, 2H), 7.41 (t, *J* = 6.9 Hz, 2H), 7.32 (s, 2H), 7.20 (t, *J* = 7.1 Hz, 1H), 7.05 (t, *J* = 7.3 Hz, 2H), 6.96 (d, *J* = 7.3 Hz, 2H), 5.14 (d, *J* = 15.1 Hz, 1H), 4.67 (d, *J* = 14.5 Hz, 1H), 4.24 (dd, J_1 = 27.0 Hz, J_2 = 11.4 Hz, 3H), 3.59 (d, *J* = 17.1 Hz, 1H), 3.27 (dd, J_1 = 13.4 Hz, J_2 = 4.1 Hz, 1H), 3.12 (d, *J* = 11.2 Hz, 1H), 2.45 (d, *J* = 17.1 Hz, 1H). ^{13}C-NMR (126 MHz, DMSO-d_6) δ: 165.97, 164.79, 162.85, 139.73, 139.20, 135.36, 133.81, 132.53, 131.00, 130.26, 129.07, 128.70, 128.26, 128.04, 127.62, 127.10, 60.98, 48.83, 48.78, 46.29, 36.88. $[\alpha]_D^{25}$ = 1.18 (1.13 mg/mL, MeOH). HR-MS (ESI, m/z): Calcd for 478.15281. ($C_{26}H_{25}ClN_3O_4^+$[M+H]$^+$). Found 478.15289.

4.1.6.11 (R)-4-((3-benzyl-4-(3-methoxybenzyl)-2, 5-dioxopiperazin-1-yl)methyl)-N-hydroxybenzamide ***(18e)*** 48.6% isolated yield; white solid. Mp: 200-202 °C; ^{1}H-NMR (500 MHz, DMSO-d_6) δ: 11.38 (s, 1H), 9.21 (s, 1H), 7.97 (s, 2H), 7.80 (d, *J* = 7.7 Hz, 2H), 7.31 (d, *J* = 7.5 Hz, 2H), 7.20 (t, *J* = 7.0 Hz, 1H), 7.06 (t, *J* = 7.2 Hz, 2H), 6.98 (d, *J* = 7.2 Hz, 2H), 6.91 (s, 2H), 5.19 (d, *J* = 15.0 Hz, 1H), 4.65 (d, *J* = 14.5 Hz, 1H), 4.26 (d, *J* = 14.5 Hz, 1H), 4.20 (s, 1H), 4.12 (d, *J* = 14.9 Hz, 1H), 3.76 (s, 3H), 3.61 (s, 1H), 3.34-3.20 (m, 1H), 3.10 (d, *J* = 11.1 Hz, 1H), 2.49 (d, *J* = 17.1 Hz, 1H). ^{13}C-NMR (126 MHz, DMSO-d_6) δ: 166.07, 164.65, 162.88, 160.03, 139.22, 138.52, 135.45, 132.52, 130.33, 130.27, 129.06, 128.69, 127.61, 120.50, 114.26, 113.33, 60.64, 56.27, 55.44, 48.82, 46.48, 36.76. $[\alpha]_D^{25}$ = −1.51 (1.02 mg/mL, MeOH). HR-MS (ESI, m/z): Calcd for 474.20235. ($C_{27}H_{28}N_3O_5^+$ [M+H]$^+$). Found 474.20245.

4.1.6.12 (S)-4-((3-((1H-indol-3-yl)methyl)-2, 5-dioxopiperazin-1-yl)methyl)-N-hydroxybenzamide ***(21a)*** 53.0% isolated yield; white solid. Mp: 198-200 °C; ^{1}H-NMR (500 MHz, DMSO-d_6) δ: 11.22 (s, 1H), 11.05 (s, 1H), 9.06 (s, 1H), 8.41 (d, *J* = 2.3 Hz, 1H), 7.61 (d, *J* = 8.2 Hz, 2H), 7.53 (s, 1H), 7.40 (d, *J* = 8.1 Hz, 1H), 7.10 (t, *J* = 7.5 Hz, 1H), 7.05 (d, *J* = 2.1 Hz, 1H), 7.00 (t, *J* = 7.4 Hz, 1H), 6.93 (d, *J* = 8.1 Hz, 2H), 4.31 (d, *J* = 3.6 Hz, 2H), 4.29-4.26 (m, 1H), 3.38 (s, 1H), 3.36 (d, *J* = 6.7 Hz, 1H), 3.08 (dd, J_1 = 14.4 Hz, J_2 = 4.3 Hz, 1H), 2.73 (d, *J* = 17.1 Hz, 1H). ^{13}C-NMR (126 MHz, DMSO-d_6) δ: 166.64, 165.11, 145.91, 139.44, 138.30, 136.48, 132.29, 128.60, 127.97, 127.57, 126.01, 125.19, 121.48, 119.20, 118.97, 111.83, 108.50, 56.14, 49.01, 48.42. $[\alpha]_D^{25}$ = 0.92 (1.20 mg/mL, MeOH). HR-MS (ESI, m/z): Calcd for 393.15573. ($C_{21}H_{21}N_4O_4^+$ [M+H]$^+$). Found 393.15594.

4.1.6.13 (R)-4-((3-((1H-indol-3-yl)methyl)-2, 5-dioxopiperazin-1-yl)methyl)-N-hydroxybenzamide ***(21b)*** 61.5% isolated yield; white solid. Mp: 189-191 °C; ^{1}H-NMR (500 MHz, DMSO-d_6) δ: 11.16 (s, 1H), 10.97 (s, 1H), 9.04 (s, 1H), 8.37 (s, 1H), 7.58 (dd, J_1= 14.2, J_2 = 7.9 Hz, 3H), 7.40 (d, *J* = 8.1 Hz, 1H), 7.11 (t, *J* = 7.5 Hz, 1H), 7.06 (s, 1H), 7.01 (t, *J* = 7.4 Hz, 1H), 6.94 (d, *J* = 7.8 Hz, 2H), 4.31 (d, *J* = 8.5 Hz, 2H), 4.29 (s, 1H), 3.43-3.38 (m, 1H), 3.20 (d, *J* = 4.8 Hz, 1H), 3.07 (dd, J_1= 14.3, J_2 = 3.7 Hz, 1H), 2.74 (d, *J* = 17.2 Hz, 1H). ^{13}C-NMR (126 MHz, DMSO-d_6) δ: 166.63, 165.14, 164.56, 139.46, 136.47, 132.33, 128.00, 127.89, 127.54, 125.19, 121.52, 119.20, 119.00, 111.80, 108.55, 56.13, 49.09, 49.01, 48.43. $[\alpha]_D^{25}$ = 2.16 (1.16 mg/mL, MeOH). HR-MS (ESI, m/z): Calcd for 393.15573. ($C_{21}H_{21}N_4O_4^+$ [M+H]$^+$). Found 393.15594.

4.2 In vitro HDAC enzymatic assay

The inhibitory activity of all HDAC isoforms except HDAC10 were conducted by the Reaction Biology Corporation, Malvern , PA using HDAC fluorescent activity assay based on the unique Fluor de Lys™ substrate and developer combination. Compounds were dissolved in DMSO and tested in at least 10-dose IC_{50} mode with 3-fold serial dilution starting at 50 μM. GraphPad Prism 5.0 software was used to calculate the IC_{50} values for each compound.

The assay for HDAC10 activity was performed in the Cancer Drug Development group at the German Cancer Research Center (69210 Heidelberg, Germany). The detailed protocol can be found in reference [30].

4.3 Western Blotting

HCT116 cells (1×10^6) were seeded overnight and then incubated with indicated concentrations of compounds for 24 h. Cell extract was prepared by lysing cultured cells with a mammalian protein extraction reagent supplemented with EDTA-free protease inhibitor for 15 min. Supernatants were collected following centrifugation of lysed cells at 15000 g for 10 min at 4 °C. To analyze the cell lysate, 30 μg of total protein per sample was resolved by SDS-PAGE and transferred onto a nitrocellulose membrane. Membranes with immobilized proteins were probed with antibodies for H3 acetylation. The reactive protein bands were visualized using an ECL detection system.

4.4 Growth Percent on 60 Cell Lines by NCI.

All detailed test method is described on the NCI Web site (https://dtp.cancer.gov/discovery_development /nci-60/methodology.htm).

4.5 In vitro cell growth inhibitory activity.

Culture medium and culture condition of cell lines. The cells were cultured in IMDM medium with 20% FBS, 100 U/mL penicillin and 100 ug/mL streptomycin. All cells were maintained at 37 °C in a humidified atmosphere of 5% CO_2 in air.

Cell Growth Inhibitory Assay. The protocol using Alamar blue reagent for antiproliferative activitives was as follows: 1. plated 100 μL cell suspension or completed medium into 96-well plate using a Matrix 12-channel pipettor. And filled residual wells with 200 μL PBS per well; 2. drugs were added to each well of 96-well plate; 3. placed plate into an incubator with corresponding culture condition for 72 h; 4. pipetted 22 μL Alamar blue solution (1 mM) into each well of 96-well plate; 5. returned plate to incubator and leave for 5~6 h; 6. shook plate for 10 seconds and recorded fluorescence at 530/590 nm.

Combination index was calculated by applying the equation $CI_{50} = IC_{50Ac}/IC_{50As} + IC_{50Bc}/IC_{50Bs}$, where IC_{50As} and IC_{50Bs} are concentrations of inhibitors A and B required to produce 50% effect when used as single agents, and IC_{50Ac} and IC_{50Bc} are concentrations of inhibitors A and B required to produce 50% effect when used in combination.

4.6 Computational Methods

All computational work was performed in Discovery Studio 3.0 software (BIOVIA, 5005 Wateridge Vista Drive, San Diego, CA92121 USA). Docking was conducted using cdocker module based on the cocrystals of human HDAC6 (PDB code: 5EDU), human HDAC1 (PDB code: 5ICN) and human HDAC8 (PDB code: 1W22). The cavities of the cocrystals occupied by their ligands were selected as the binding sites. Key waters molecules in the binding pocket were reserved. The energy minimization for compound was performed by Powell's method for 1000 iterations using tripos force field and with Gasteiger-Hückel charge. The other docking parameters were kept as default.

4.7 Microsomal stability assay

Human liver microsome was purchased from Research Institute for Liver Disease (Shanghai) Co., Ltd. NADPH was purchased from Roche. The assay was as follows: each incubated mixture contained 0.8 mg/mL human liver microsome, 50 μL magnesium chloride, 60 μL potassium phosphate buffer (pH 7.4) and 0.5 μM test compound in a total volune of 200 μL. After prewarming at 37 °C for 5 min, 50 μL NADPH was added to initiate the reaction. The reaction was terminated after 0, 5, 10, 15, 30, 60 or 90 min by adding 400 μL ice-cold ethyl acetate into 200 μL of incubation mixture. The sample was then centrifuged at 4000 rpm for 10 min at 4 °C. The supernatant was then analyzed by LC−MS/MS.

Acknowledgment

We thank the NCI Division of Cancer Treatment & Diagnosis for the NCI-60 screening of our compounds. This work was supported by the National Natural Science Foundation of China (81903464 and 21503168), Chinese Universities Scientific Fund (2452017174) and the Natural Science Foundation of Jiangsu Province (BK20180573).

Appendix A. Supplementary data

Supplementary data related to this article can be found at

References

[1] Minucci, S.; Pelicci, P. G., Histone deacetylase inhibitors and the promise of epigenetic (and more) treatments for cancer, Nat. Rev. Cancer 6 (1) (2006), 38-51.

[2] Chen X.; Zhao S.; Li H. M.; Wang X.; Geng A. X.; Cui H.; Lu T.; Chen Y. D.; Zhu Y. Eur. J. Med. Chem. 168 (2019), 110-122.

[3] Piekarz, R.; Bates, S., A review of depsipeptide and other histonedeacetylase inhibitors in clinical trials. Curr. Pharm. Des. 10 (19) (2004), 2289-2298.

[4] Marks, P. A.; Xu, W. S., Histone deacetylase inhibitors: potential in cancer therapy. J. Cell. Biochem. 107 (4) (2009), 600-608.

[5] Fraczek, J.; Vanhaecke, T.; Rogiers, V., Toxicological and metabolic considerations for histone deacetylase inhibitors. Expert Opin. Drug Metab. Toxicol. 9 (4) (2013), 441-457.

[6] Witt, O.; Deubzer, H. E.; Milde, T.; Oehme, I., HDAC family: What are the cancer relevant targets? Cancer Lett. 277 (1) (2009), 8-21.

[7] Best, J. D.; Carey, N., Epigenetic therapies for non-oncology indications. Drug Discovery Today 15 (2010), 1008-1014.

[8] Govindarajan, N.; Rao, P.; Burkhardt, S.; Sananbenesi, F.; Schluter, O. M.; Bradke, F.; Lu, J. R.; Fischer, A., Reducing HDAC6 ameliorates cognitive deficits in a mouse model for Alzheimer's disease. EMBO. Mol. Med. 5 (1) (2013), 52-63.

[9] Asthana, J.; Kapoor, S.; Mohan, R.; Panda, D., Inhibition of HDAC6 deacetylase activity increases its binding with microtubules and suppresses microtubule dynamic instability in MCF-7 cells. J. Biol. Chem. 288 (31) (2013), 22516-22526.

[10] Kekatpure, V. D.; Dannenberg, A. J.; Subbaramaiah, K., HDAC6 modulates Hsp90 chaperone activity and regulates activation of aryl hydrocarbon receptor signaling. J. Biol. Chem. 284 (12) (2009), 7436-7445.

[11] Zhang, X. H.; Yuan, Z. G.; Zhang, Y. T.; Yong, S.; Salas-Burgos, A.; Koomen, J.; Olashaw, N.; Parsons, J. T.; Yang, X. J.; Dent, S. R.; Yao, T. P.; Lane, W. S.; Seto, E., HDAC6 modulates cell motility by altering the acetylation level of cortactin. Mol. Cell 27 (2) (2007), 197-213.

[12] Kalin J. H.; Bergman J. A., Development and therapeutic implications of selective histone deacetylase 6 inhibitors. J. Med. Chem. 56 (16) (2013), 6297-6313.

[13] Siedel, C.; Schnekenburger, M.; Dicato, M.; Diederich, M., Histone deacetylase 6 in health and disease. Epigenomics 7 (1) (2015), 103-118.

[14] Yang, P. H.; Zhang, L.; Zhang, Y. J.; Zhang, J.; Xu, W. F. HDAC6: Physiological function and its selective inhibitors for cancer

treatment. Drug Discoveries Ther. 7 (6) (2013), 233-242.

[15] Santo, L.; Hideshima, T.; Kung, A. L.; Tseng, J. C.; Tamang, D.; Yang, M.; Jarpe, M.; Van Duzer, J. H.; Mazitschek, R.; Ogier, W. C.; Cirstea, D.; Rodig, S.; Eda, H.; Scullen, T.; Canavese, M.; Bradner, J.; Anderson, K. C.; Jones, S. S.; Raje, N., Preclinical activity, pharmacodynamic, and pharmacokinetic properties of a selective HDAC6 inhibitor, ACY-1215, in combination with bortezomib inmultiple myeloma. Blood 119 (11) (2012), 2579-2589.

[16] Lee J. H.; Mahendran A.; Yao Y.; Ngo L.; Venta-Perez G.; Choy M. L.; Kim N.; Ham WS, Breslow R, Marks PA., Development of a histone deacetylase 6 inhibitor and its biological effects. Proc Natl Acad Sci U S A. 110 (39) (2013), 15704-15709.

[17] Kyle V. Butler; Jay Kalin; Camille Brochier; Guilio Vistoli; Brett Langley; Alan P. Kozikowski, Rational Design and Simple Chemistry Yield a Superior, Neuroprotective HDAC6 Inhibitor, Tubastatin A. J. Am. Chem. Soc. 132 (31) (2010), 10842-10846.

[18] Wang X. X.; Wan R. Z.; Liu Z. P., Recent advances in the discovery of potent and selective HDAC6 inhibitors. Eur. J. Med. Chem. 143 (2018), 1406-1418.

[19] Nepali K.; Lee H. Y.; Lai M. J.; Ojha R.; Wu T. Y.; Wu G. X.; Chen M. C.; Liou J. P., Ring-opened tetrahydro-γ-carbolines display cytotoxicity and selectivity with histone deacetylase isoforms. Eur. J. Med. Chem. 127 (2017), 115-127.

[20] Lee H. Y.; Tsai A. C.; Chen M. C.; Shen P. J.; Cheng Y. C.; Kuo C. C.; Pan S. L.; Liu Y. M.; Liu J. F.; Yeh T. K.; Wang J. C.; Chang C. Y.; Chang J. Y.; Liou J. P., Azaindolylsulfonamides, with a more selective inhibitory effect on histone deacetylase 6 activity, exhibit antitumor activity in colorectal cancer HCT116 cells. J. Med. Chem. 57 (10) (2014), 4009-4022.

[21] Furumai R.; Matsuyama A.; Kobashi N.; Lee K. H.; Nishiyama M.; Nakajima H.; Tanaka A.; Komatsu Y.; Nishino N.; Yoshida M., Horinouchi S. FK228 (depsipeptide) as a natural prodrug that inhibits class I histone deacetylases. Cancer Res. 62(17) (2002), 4916-4921.

[22] Watson P. J.; Millard C. J.; Riley A. M.; Robertson N. S.; Wright L. C.; Godage H. Y.; Cowley S. M.; Jamieson A. G.; Potter B. V.; Schwabe J. W., Insights into the activation mechanism of class I HDAC complexes by inositol phosphates. Nat. Commun. 7 (2016), 11262.

[23] Krieger V.; Hamacher A.; Gertzen C. G. W.; Senger J.; Zwinderman M. R. H.; Marek M.; Romier C.; Dekker F. J.; Kurz T.; Jung M.; Gohlke H.; Kassack M. U.; Hansen F. K., Design, Multicomponent Synthesis, and Anticancer Activity of a Focused Histone Deacetylase (HDAC) Inhibitor Library with Peptoid-Based Cap Groups. J. Med. Chem. 60 (13) (2017), 5493-5506.

[24] Bhatia S.; Krieger V.; Groll M.; Osko J. D.; Reßing N.; Ahlert H.; Borkhardt A.; Kurz T.; Christianson D. W.; Hauer J.; Hansen F. K., Discovery of the First-in-Class Dual Histone Deacetylase–Proteasome Inhibitor. J. Med. Chem. 61 (22) (2018), 10299-10309.

[25] Nicholas J., David W., Christianson; Binding of the Microbial Cyclic Tetrapeptide Trapoxin A to the class I Histone Deacetylase HDAC8. ACS Chem. Biol. 12 (9) (2017), 2281-2286.

[26] Wang D.; Li W.; Zhao R.; Chen L.; Liu N.; Tian Y.; Zhao H.; Xie M.; Lu F.; Fang Q.; Liang W.; Yin F.; Li Z., Stabilized peptide HDAC inhibitors derived from HDAC1 substrate H3K56 for the treatment of cancer stem-like cells in vivo. Cancer Res. 79(8) (2019),1769-1783.

[27] Lin X.; Chen W.; Qiu Z.; Guo L.; Zhu W.; Li W.; Wang Z.; Zhang W.; Zhang Z.; Rong Y.; Zhang M.; Yu L.; Zhong S.; Zhao R.; Wu X.; Wong J. C.; Tang G., Design and synthesis of orally bioavailable aminopyrrolidinone histone deacetylase 6 inhibitors. J Med Chem. 58(6) (2015), 2809-2820.

[28] Lee H. Y.; Nepali K.; Huang F. I.; Chang C. Y.; Lai M. J.; Li Y. H.; Huang H. L.; Yang C. R.; Liou J. P.; (*N*-Hydroxycarbonylbenylamino)quinolines as selective histone deacetylase 6 inhibitors suppress growth of multiple myeloma in vitro and in vivo. J Med Chem. 61(3) (2018), 905-917.

[29] Vögerl K.; Ong N.; Senger J.; Herp D.; Schmidtkunz K.; Marek M.; Müller M.; Bartel K.; Shaik T. B.; Porter N. J.; Robaa D.; Christianson D. W.; Romier C.; Sippl W.; Jung M.; Bracher F., Synthesis and biological investigation of phenothiazine-based benzhydroxamic acids as selective histone deacetylase 6 inhibitors. J. Med. Chem. 62(3) (2019), 1138-1166.

[30] Borthwick, A. D., 2,5-Diketopiperazines: synthesis, reactions, medicinal chemistry, and bioactive natural products. Chem Rev. 112 (7) (2012), 3641-716.

[31] Géraldy M.; Morgen M.; Sehr P.; Steimbach R. R.; Moi D.; Ridinger J.; Oehme I.; Witt O.; Malz M.; Nogueira M. S.; Koch O.; Gunkel N.; Miller A. K., Selective Inhibition of Histone Deacetylase 10: Hydrogen Bonding to the Gatekeeper Residue is Implicated. J

Med Chem. 62(9) (2019), 4426-4443.

[32] Porter N. J.; Mahendran A.; Breslow R.; Christianson D. W., Unusual zinc-binding mode of HDAC6-selective hydroxamate inhibitors. Proc Natl Acad Sci U S A. 114(51) (2017), 13459-13464.

[33] Porter N. J.; Osko J. D.; Diedrich D.; Kurz T.; Hooker J. M.; Hansen F. K.; Christianson D. W., Histone Deacetylase 6-Selective Inhibitors and the Influence of Capping Groups on Hydroxamate-Zinc Denticity. J. Med. Chem. 61(17) (2018), 8054-8060.

HIGHLIGHTS

- Potent and highly selective HDAC6 inhibitors based on the natural 2, 5-diketopiperazine scaffold.
- Computational simulations suggested the key interactions between DKPs and HDAC6.
- Combination of **18a** and adriamycin exhibited synergistic antiproliferative influence on A549 cell.

Declaration of interests

☐The authors declare that they have no known competing financial interests or personal relationships that could have appeared to influence the work reported in this paper.